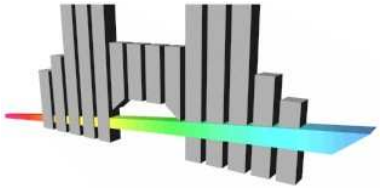

U.C. Berkeley

Imaging system of a Bose-Einstein Condensation experiment

Fabien Lienhart

September 4, 2003

Contents

Introduction

I spent the four last months in Pr. Stamper-Kurn's team in the Physics department of U.C. Berkeley. I worked on the installation of an imaging system on a Bose-Einstein Condensation experiment, and its use was made as easy as possible, by developing automation routines on the computer which controled the device.Though my application period finishes only in one month, this report will introduce what has already been achieved during these first months, and what I plan to finalize in the following month.

In a first part I will present the Bose-Einstein condensation phenomenon, how it can be theoretically predicted, and it can be experimentally realized. This part aims to explain the basics of Bose-Einstein Condensation. Therefore it is taken from different books, lectures and websites. People which are already familiar with the subject should skip it, as nothing in it was done on my own.

The second part focuses on the imaging system I am building. After a brief explanation of the different imaging techniques leading to quantitative measurement, I will present the experimental device, explain why a test pattern has to be used to characterize the system, how this is achieved, and I will finally produce my results.

The last part is dedicated to the automation procedures I developed in Visual Basic: the routines were created to save time in the most used imaging processes, such as taking an absorption image, saving the images, or rotating them. I will review all the programs developed.

Chapter 1

Introduction to Bose-Einstein condensation

In 1924-1925, Albert Einstein and Satyenda Nath Bose predicted that a phase transition had to be expected from a boson gas cooled under a critical temperature T_c. Indeed, below T_c, a macroscopic number of atoms in the ground level should be observed. As the increasing number of atoms in this state should suddenly increase the density of the gas, the transition is, in some way, similar to the condensation of a gas into a liquid. Hence the name given to this transition: Bose-Einstein condensation. It took 70 years for scientists to give experimental evidence of the phenomenon: it was achieved for the first time in 1995 by Eric Cornell and Carl Wieman in Boulder, Colorado.

In this part, we will first give a simple demonstration of the Bose-Einstein Condensation. Then, we will focus on the description of the experimental apparatus.

1.1 Prediction of the phenomenon

We will here briefly retranslate the derivation made by Claude Cohen-Tannoudji in his lectures at the *College de France* [4], limiting our study to atoms freely evolving.

Let us consider a gas of bosons without mutual interactions enclosed in a cubic box of length L and volume V, in thermodynamic equilibrium at temperature T. In order to make things easier, periodic limit conditions are taken.

The momentum of each particle is quantified $p_i = \dfrac{2\pi\hbar}{L} n_i \ , \qquad i = x, y, z$

The energy of an atom is thus: $\epsilon_p = \dfrac{2\pi^2\hbar^2}{mL^2}(n_x^2 + n_y^2 + n_z^2)$, the energy of the ground state is $\epsilon = 0$, and the energy difference between the first excited state and the ground state is

$$\delta\epsilon = \frac{2\pi^2\hbar^2}{mL^2} \tag{1.1}$$

We will see later that BEC (Bose-Einstein Condensate) appears at a temperature T_c such that $kT_c \gg \delta\epsilon$. The BEC is hence not due to the fact that thermal energy is of the same order of magnitude (or smaller) than the difference of energy between the ground and the excited states.

The density of state can then be easily calculated using the approximation of the continuous spectrum, by which the summation on the possible values of the momentum is transformed into an integral. The density of state is: $\rho(x) = \dfrac{V}{\lambda_{dB}^3}\dfrac{2}{\sqrt{\pi}}\sqrt{x}$, where $x = \beta\epsilon = \dfrac{\epsilon}{kT}$ and $\lambda_{dB} = \sqrt{\dfrac{2\pi\hbar^2}{mkT}}$

is the de Broglie wavelength[1].

For μ and T constant, the mean occupation number can be calculated with the grand partition function:

$$\overline{N_p} = \frac{1}{e^{\beta(\epsilon_p - \mu)} - 1} = \frac{1}{z^{-1}e^{\beta\epsilon_p} - 1} \tag{1.2}$$

where $z = e^{\beta\mu}$ is the fugacity and μ the chemical potential. An important thing to note is that μ is such that $\forall p,\ \epsilon_p - \mu > 0$, in other words $\forall p,\ \epsilon_0 - \mu > 0$, otherwise N_p could be negative[2]. In our particular case, it implies that $\mu < 0$ and thus $z < 1$.

Let us now consider another problem which is: given a fixed number of bosons N in equilibrium at temperature T, how will vary the repartition of the molecules between the levels ϵ_p when T is changed? If fluctuations of the number of particles around their average values are ignored, results of the grand canonical ensemble can be used to write:

$$N = \sum_p \overline{N_p} = \sum_p \frac{1}{z^{-1}e^{\beta\epsilon_p} - 1} \tag{1.3}$$

To do this calculation, one will, in a first time, try to use once more the approximation of coninuous spectrum. Thus,

$$\begin{aligned} N &= \int_0^\infty dx\ \rho(x)\frac{1}{z^{-1}e^{\beta\epsilon_p} - 1} && (1.4)\\ &= \frac{V}{\lambda_{dB}^3}\frac{2}{\sqrt{\pi}}\int_0^\infty dx\ \sqrt{x}\frac{ze^{-x}}{1 - ze^{-x}} && (1.5)\\ &= \frac{V}{\lambda_{dB}^3}g_{3/2}(z) && (1.6) \end{aligned}$$

where $g_{3/2}(z) = \sum_{l=1}^{\infty}\frac{z^l}{l^{3/2}}$ is the Bose function. It is strictly increasing from $g_{3/2}(0) = 0$ to $g_{3/2}(1) = 2.612$.

The problem is that z cannot be greater than 1, so the integral cannot be greater than 2.612, hence the latter equation has no solution if:

$$\begin{aligned} N &\geq 2.612\ \frac{V}{\lambda_{dB}^3} && (1.7)\\ n\lambda_{dB}^3 &\geq 2.612 && (1.8) \end{aligned}$$

where $n = N/V$ is the density of atoms. This problem arose from the approximation of continuous spectrum in which the ground state has a density $\rho(0) = 0$. The population $\overline{N_0}$ has been neglected in our calculation, which is not bothering as long as the population of this state is equivalent to the one of the many others. But if $\overline{N_0}$ becomes macroscopic, it has to be taken into account in the expression of N.

$$\begin{aligned} N &= \overline{N_0} + \frac{V}{\lambda_{dB}^3}g_{3/2}(z) && (1.9)\\ &= \frac{z}{1 - z} + \frac{V}{\lambda_{dB}^3}g_{3/2}(z) && (1.10) \end{aligned}$$

[1] De Broglie wavelength can be seen as the extension of the particle given by its ondulatory nature as a function of the temperature: at high T, λ_{dB} is small compared with its material size and thus the quantum behavior of the particle is totally negligible, but as T is cooled down, λ_{dB} increases, meaning that the quantum nature of the atom has gains in importance, and will ultimately have to be taken into account.

[2] A better demonstration of that result can be found in statistical physics books[7]: the grand partition function Z for a boson gas can be considered as the product $Z = \prod_{i=1}^{\infty} Z_i$ of partial partition functions $Z_i = \sum_{n_i} e^{\beta(\mu - \epsilon_i)n_i}$, and Z_i can converge only if $\forall i,\ \mu - \epsilon_i < 0$.

The condensation phenomenon Starting from a high T, λ_{dB} will be very small compared to the mean distance between particles $n^{1/3}$. The equation (1.10) of N has a solution with a negligible first term.
But as T decreases, λ_{dB} increases, up to $T = T_c$, where $n\lambda_{dB}^3 = 2.612$. Using the expression of de Broglie wavelength, T_c can be expressed:

$$kT_c = \frac{2\pi\hbar^2}{m}\left(\frac{n}{2.612}\right)^{2/3} \tag{1.11}$$

The second term of the equation (1.10) can be equal to N for the maximum value of z, $z = 1$. When $T < T_c$, even for $z = 1$, the second term cannot equal N, the first term (the population of the ground state) furnishes the missing *macroscopic* population.

Conclusion: for a fixed number N of atoms in the system, as T decreases, a macroscopic population $\overline{N_0}$ condenses in the ground state when $T < T_c$. And the Bose-Einstein condensation is born!

Variation of N_0 with T By definition of T_c, $N = \dfrac{V}{\lambda_{dB}^3(T_c)} g_{3/2}(1)$
Moreover, for $T < T_c$, one can write: $N = N_0 + \dfrac{V}{\lambda_{dB}^3} g_{3/2}(1)$,
so that, substituting $V g_{3/2}(1)$ from the former to the latter equation, one gets:

$$N = N_0 + \left[\frac{\lambda_{dB}^3(T_c)}{\lambda_{dB}^3(T)}\right]^3 N \tag{1.12}$$

$$= N_0 + \left(\frac{T}{T_c}\right)^{3/2} N \tag{1.13}$$

$$\boxed{\frac{N_0}{N} = 1 - \left(\frac{T}{T_c}\right)^{3/2}} \qquad \text{for } T \leq T_c$$

Comparison of kT_c with the difference between the energy levels $\delta\epsilon$ Using the former equations for $\delta\epsilon$ and kT_c, respectively (1.1) and (1.11), one gets:

$$\frac{\delta\epsilon}{kT_c} \sim \frac{n^{-2/3}}{L^2} = \frac{1}{L^2}\left(\frac{N}{L^3}\right)^{-2/3} = \frac{1}{N^{2/3}} \ll 1 \tag{1.14}$$

Thus, Bose-Einstein condensation appears for temperatures T_c much higher than $\delta\epsilon/k$. For example, for $N \sim 10^6$, $kT_c \sim 10^4\delta\epsilon$

Population of the first excited levels below the condensation threshold Let us compare N_0 to the population of the first excited level N_1 when N_0 reaches a macroscopic value, such as $N_0 = N/2$.

$$N_0 = \frac{z}{z-1} = \frac{N}{2} \quad \longrightarrow \quad z \simeq 1 - \frac{2}{N} \tag{1.15}$$

As $\delta\epsilon \ll kT$, $e^{-\beta\epsilon_1} \simeq 1 - \beta\ \delta\epsilon$. Thus,

$$N_1 = \frac{ze^{-\beta\epsilon_1}}{1 - ze^{-\beta\epsilon_1}} \sim \frac{1}{1 - (1 - \frac{2}{N})(1 - \beta\ \delta\epsilon)} \sim \frac{1}{\frac{2}{N} + \beta\ \delta\epsilon} \tag{1.16}$$

Moreover, equation (1.14) leads to $\beta\ \delta\epsilon \sim N^{-2/3}$. Hence, $\beta\ \delta\epsilon \gg \frac{2}{N}$ and so

$$\frac{N_1}{N_0} \sim \frac{1}{\beta\ \delta\epsilon\ N} \sim \frac{N^{2/3}}{N} \sim \frac{1}{N^{1/3}} \ll 1 \tag{1.17}$$

Below the condensation threshold, the population of the ground level is much higher than the one of the first excited level.

Conclusion A gas of N bosons without mutual interaction, enclosed in a box, will condense under a given temperature T_c. This condensation is not due to the fact that the temperature reached is smaller than the difference between the first energy levels, but anyway the ground state will be macroscopically populated following the law:

$$\frac{N_0}{N} = 1 - \left(\frac{T}{T_c}\right)^{3/2} \quad \text{for } T < T_c \quad \text{with} \quad kT_c = \frac{2\pi\hbar^2}{m}\left(\frac{n}{2.612}\right)^{2/3} \tag{1.18}$$

1.2 The experimental device

The apparatus used by the Stamper-Kurn's group will now be described. Atoms of ^{87}Rb were heated in an oven, producing a fine flow of Rubidium in a vacuum chamber. The trapping and the cooling of the atoms can be splitted in 5 parts:

Zeeman Slowing Atoms propagate in a 2-meter long tube. A counterpropagating laser slows them by radiation pressure. In order to stay on resonance with the slowed atom whose Doppler-shift changes, a magnetic field varies in strength along the path of the atoms, so that the Zeeman shift maintains the atoms on resonance with the laser. Coming out of the oven, their velocity is about 400 m/s. After the slowing, the mean speed is about 10 m/s.

Magneto-Optical Trapping Atoms then fly to the center of the vacuum chamber[3] where they are trapped and cooled further by an optical molasses: 6 counterpropagating lasers keep the atoms in the center of the room, thanks to a magnetic field which, once again, Zeeman-shifts the atoms trying to escape from the trap, putting them to resonance with the laser they are approaching.

Polarization Gradient Cooling The magnetic field is shut down. The atomic cloud expands. But as the counterpropagating lasers form a sinusoidal grating, and every time an atom "climbs up" the potential, it is pumped down by a laser to the bottom of the sinusoid, so that the atom always climbs up an infinite dielectric potential. This step only lasts a few milliseconds but cools the atoms below 100 μK

Magnetic Trapping After a few ms polarization gradient cooling, a spherical magnetic field is suddenly increased to trap the atoms. Because only the $m_F = -1$ state can be trapped, two third of the cloud are lost in this step. The magnetic field is then adiabatically curved to give the cloud a cigare shape.

Evaporative cooling This last step consists in broadcasting radiofrequency tuned on the transition frequency of the hottest atoms in the cloud. These one will change their polarizations so that they don't see any confining potential and escape the trap. Getting rid of the hottest

[3] During my internship, we unfortunately were forced to open the vacuum chamber, because of a leaquage in the cooling system of the coils. This was the opportunity for me to discover the vacuum techniques. A quick appendix is dedicated to them at the end of the report.

atoms, and after rethermalization, the cloud will be colder. The radio-frequency are slowly swept to progressively cool further the atoms. After the evaporative cooling a fraction of the atomic cloud should have condensed to the ground state.

I will describe more in detail each step of the experiment before summarizing what was achieved during the last four months.

1.2.1 The Slower

Rubidium atoms are first heated at $\sim 500\ K$ to get a vapor of Rb. The atoms enter the vacuum system trough a small aperture controlled by a shutter. A rubidium jet propagates then along a 2-meter channel at very high velocity (around $300\ m/s$, but the distribution is very spread out). To slow it, a laser beam is sent in the opposite direction of the jet: atoms absorb a photon with a momentum pointing in the opposite direction of their motion. A stimulated emission will emit a photon in the same direction as the laser, and finally the atom will not have lost any momentum in such cycle. But as the spontaneous emission is isotropic, the average momentum of the emitted photons on many spontaneous emission is 0. Hence, after many absorption-spontaneous emission cycles, the atoms will be slowed down.

Because of the Doppler-shift, the atoms "see" a blue-detuned laser frequency. In order to be on resonance with the $|F = 2 > \rightarrow |F' = 3 >$ transition[4], the laser must be red-detuned. The detuning of the laser gives the highest velocity which will be slowed down in the slower. In our case, the detuning is $-563\ MHz$. It corresponds to a maximum velocity:

$$v = c\frac{\Delta f}{f} = \lambda \Delta f \tag{1.19}$$

$$\simeq 780.10^{-9} \times 563.10^{6}\ m/s = \underline{440\ m/s} \tag{1.20}$$

Any atom coming out from the oven with a greater velocity will not be slowed down.

As they progress into the channel, the atoms are slowed and thus their Doppler-shift changes, so that, if nothing is done, they are rapidly out of resonance. To cope for the loss of Doppler-shift, a strong Magnetic field is along the axis, which grows almost exponentially with the distance to the oven, starting from $B = 0\ G$ at the oven, up to $G \simeq 260\ G$ at the end of the path. This is achieved by wrapping copper wires around the channel, and by increasing the density of loops when the end of the channel approaches.

Let us give an evaluation of the final velocity.

$$Red\ detuning = Doppler\ Shift + Zeeman\ Shift \tag{1.21}$$

$$2\pi\hbar f_{rd} = \mu_B \Delta(g_F m_F)B + 2\pi\hbar\frac{v}{\lambda} \tag{1.22}$$

Hence,

$$v = \lambda\left[f_{rd} - \frac{\mu_B \Delta(g_F m_F)B}{h}\right] \tag{1.23}$$

$$\simeq 780.10^{-9}\left[563.10^{-6} - \frac{1.4.10^{6} * 260}{6.62.10^{-34}}\right] \tag{1.24}$$

$$\simeq \underline{150\ m/s} \tag{1.25}$$

[4]For precisions about the transitions, the reader should refer to the appendix dedicated to ^{87}Rb spectroscopy. Let us just mention that $|F >$ states are the ground states and $|F' >$ are excited.

1.2.2 The Magneto-Optical Trap

After a short time of flight, the atoms arrive at the center of the chamber and fall into a Magneto-Optical Trap (MOT). We will first decribe it in 1 dimension, and see it can be easily generalized to 3D.

1-Dimension model A 1D MOT is made of two counterpropagating lasers of different polarizations (σ^+ and σ^-) both slightly red-detuned ($\sim$ 8 MHz), and a linear magnetic field $B(z) = A.z$. We will consider the simple scheme of an atomic transition of $J_g = 0 \rightarrow J_e = 1$. The excited state has thus 3 Zeeman sublevels which will be proportionaly shifted with the field. Assuming the lasers and the magnetic field are as in figure 1.1, when an atom in the ground state moves to the right, its $|J_e, M_e = -1 >$ state shifts down to the laser frequency. A photon from the σ^- beam is then absorbed, and the atom is pushed toward the center of the MOT. On the other side of the center of the trap, analogous phenomenons occur with the σ^+ beam and the $M_e = +1$ sublevel.

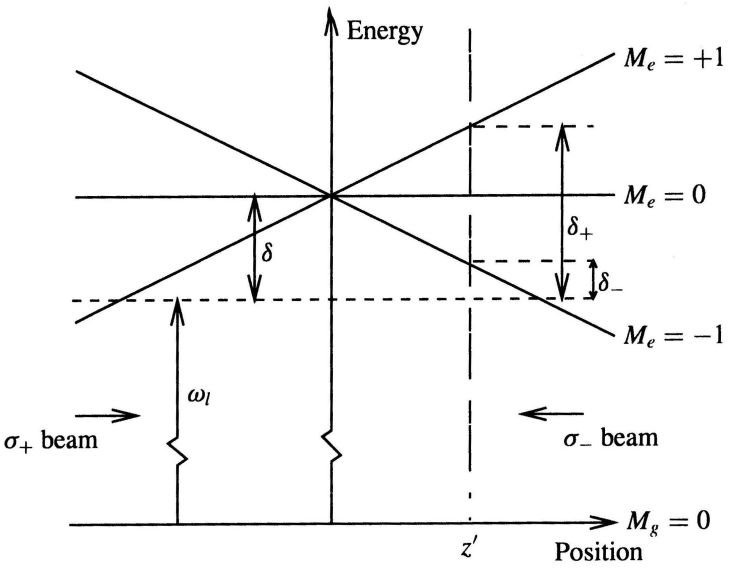

Figure 1.1: Arrangement for a unidimensional MOT. The horizontal dashed line represents the laser frequency seen by an atom at rest in the center of the trap. Because of the Zeeman shifts of the atomic transition frequencies in the homogeneous magnetic field, atoms at $z = z'$ are closer to resonance with the σ^- laser beam than with the σ^+ one, and are therefore driven toward the center of the trap. Figure taken from [9].

The MOT scheme can easily be extended to 3D by using six instead of two laser beams (see figure 1.2). Things are a little bit more complicated in our case, as the "ground" state has different Zeeman sublevels. However things will not be dramatically changed, as σ^+ laser beam will pump the atoms to the $M_g = +J_g$ substate, which forms a closed system with the $M_e = +J_e$ substate (see Appendix A).

Trapping AND Cooling It is important to note that, contrary to the Magnetic trap we will study later, the MOT cools down the atoms. It can be showed by writing the radiative force in

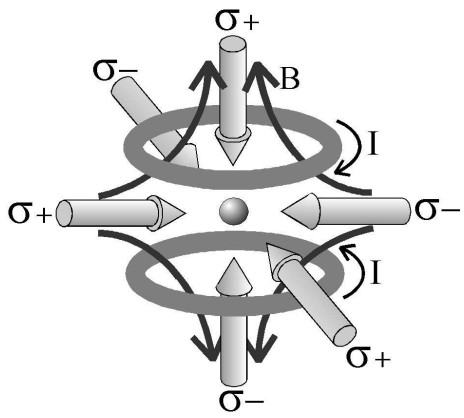

Figure 1.2: A tri-dimensional Magneto-Optical Trap. Figure taken from [14]

the low intensity limit[5]. The total force on the atoms is given by:

$$\overrightarrow{F} = \overrightarrow{F}_+ + \overrightarrow{F}_- \qquad \text{where} \quad \overrightarrow{F}_\pm = \pm\frac{\hbar\overrightarrow{k}\gamma}{2}\frac{s_0}{1+s_0+(2\delta_\pm/\gamma)^2} \tag{1.26}$$

In our case, the detuning $\delta_\pm$ for each laser is given by the contribution of Doppler and Zeeman shifts:

$$\delta_\pm = \delta \mp \overrightarrow{k}\cdot\overrightarrow{v} \pm \frac{\mu_B\Delta(g_F m_F)B}{\hbar} \tag{1.27}$$

When both Doppler and Zeeman shifts are small compared to the detuning δ, the denominator of the force can be expanded. The result becomes:

$$\overrightarrow{F} = -\beta\overrightarrow{v} - \kappa\overrightarrow{r} \tag{1.28}$$

The force leads to damped harmonic motion of the atoms in the trap.

Repump laser Though cooling and trapping is achieved using the $|F=2, m_F=2> \rightarrow |F'=3, m_F=3>$ cycling transition, another excited hyper-fine state $|F'=2>$is close by, and only a small excitation rate to that state leads to a loss of atoms caused by spontaneous emission to the $|F=1>$ ground state. Since the hyperfine splitting in the ground state is very large, atoms are confined to this state and are no longer cooled and trapped. In order to prevent this, a second laser beam, called repump laser is tuned to the $|F=1> \rightarrow |F'=2>$ transition. The excited atom can then decay to the original $|F=2>$ state.

Doppler limit What temperatures can be reached with such process? Every time an atom absorbs a photon, its energy changes of $E_r = \hbar^2k^2/2M = \hbar\omega_r$. This energy is then released by the atom which recoils. This recoil leads to heating the cloud, and the limit of cooling of the method can be found by equating the rates of heating and of cooling.

Another instructive way to determine the limit temperature T_D (where D stands for Doppler) is to consider that all the spontaneous emissions of an atom cause a random walk in momentum space with step size $\hbar k$ and step frequency 2γ, where the factor of 2 arises because of the 2 beams. The random walk results in diffusion in momentum space with diffusion coefficient

[5]It means that stimulated emission has been neglected emission. For further explanations, see [9].

$D_0 \equiv 2\frac{(\Delta p)^2}{\Delta t} = 4\gamma(\hbar k)^2$. Then Brownian motion theory gives the steady-state temperature in terms of the damping coefficient β: $k_B T = D_0/\beta$. Calculations finally give the Doppler limit:

$$T_D = \frac{\hbar\gamma}{2k_B} \approx 100\ \mu K \tag{1.29}$$

However, temperature below T_D were observed in a MOT. This phenomenon is due to the cooling described in the following part: the Polarization Gradient cooling.

1.2.3 Polarization-Gradient Cooling

We will first study the linear $\perp$ linear polarization gradient cooling, and then focus on our system, working on $\sigma^+\sigma^-$ polarization gradient cooling.

Linear $\perp$ Linear polarization gradient cooling or Sisyphus effect Let us consider two counterpropagating lasers with orthogonal linear polarization. The polarization of this light field varies over half a wavelength, as shown in figure 1.3:

$$\begin{aligned} \overrightarrow{E} &= E_0\overrightarrow{x}\cos\omega_l t - kz + E_0\overrightarrow{y}\cos\omega_l t + kz & (1.30)\\ &= E_0\left[(\overrightarrow{x}+\overrightarrow{y})\cos\omega_l t\cos kz + (\overrightarrow{x}-\overrightarrow{y})\sin\omega_l t\sin kz\right] & (1.31)\end{aligned}$$

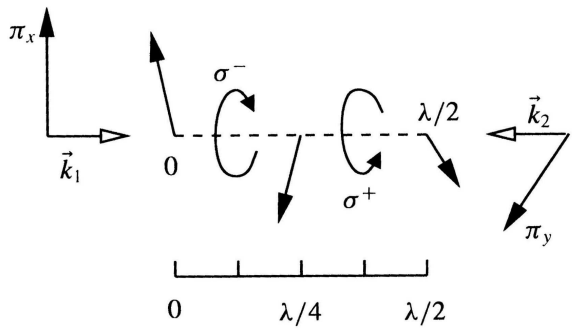

Figure 1.3: Polarization gradient field for the lin $\perp$ lin polarization. Figure taken from [9].

To study the effects of this polarization gradient on the cooling process, we will study a $J_g = 1/2$ to $J_e = 3/2$ transition as it is one of the simplest transitions showing sub-Doppler cooling.

Let us start from an atom at a position where the light is σ^+-polarized, as shown at the lower left of figure 1.4. The light optically pumps it to the negative light-shifted $m_g = +1/2$ state. In moving through the light field, the atom increases its potential energy (decreasing by the way its kinetic energy). After traveling a distance $\lambda/4$, it arrives at a position where the light field is σ^--polarized, and is optically pumped down to $m_g = -1/2$. Again the moving atom is at the bottom of a hill.

In climbing the hills, the kinetic energy is converted to potential energy, and in the optical pumping process, the potential energy is radiated away because the spontaneous emission is at a higher frequency than the absorption. Thus atoms seem to be always climbing a hill, just like the Greek hero Sisyphus.

This cooling process is effective over a limited range of atomic velocities. The damping is maximum for atoms that undergo one optical pumping process while traveling over a $\lambda/4$ distance. The optimum velocity is thus $v_c \sim \gamma/k$. Slower atoms will not reach the hilltop before

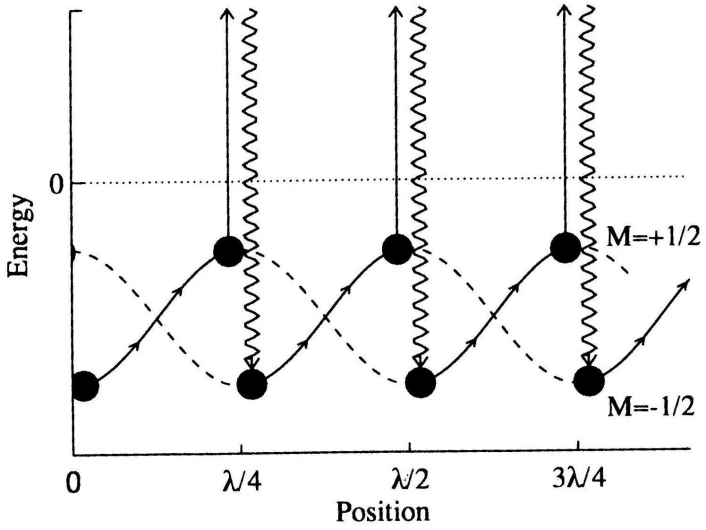

Figure 1.4: The spatial dependence of the light shifts of the ground-state sublevels of the $J = 1/2 \rightarrow 3/2$ transition for the lin $\perp$ lin polarization. The arrows show the path followed by atoms being cooled. Atoms starting up at $z = 0$ in the $m_g = +1/2$ sublevel must climb the potential hill/ As they approach the $z = \lambda/4$ point where the light becomes σ^--polarized, they are optically pumped to the $m_g = -1/2$ sublevel. They must then begin climbing another hill toward the $\lambda/2$ point, where light is σ^+-polarized, and they are pumped back to the $m_g = +1/2$ substate. The process repeats until the atomic kinetic energy is too small to climb next hill. Each optical pumping results in absorption of light at a lower frequency than emission, thus dissipating energy to the radiation field. Figure taken from [9].

the pumping process occurs, and faster atoms will already be descending the hill before being pumped toward the other sublevel. In both cases the energy loss is smaller, the cooling process less efficient.

σ^+-σ^- polarization gradient cooling This case corresponds to our experiment: two counterpropagating laser beams with σ^+ and σ^- polarizations. The resulting optical field has a constant magnitude and is linearly polarized everywhere, but direction rotates of 2π over one optical wavelength (see figure 1.5).

$$\begin{aligned} \overrightarrow{E} &= E_0\ [\overrightarrow{x}\cos(\omega_l t - kz) + \overrightarrow{y}\sin(\omega_l t - kz)] \\ &+ E_0\ [\overrightarrow{x}\cos(\omega_l t + kz) - \overrightarrow{y}\sin(\omega_l t + kz)] \qquad (1.32) \\ &= 2E_0\cos\omega_l t\ [\overrightarrow{x}\cos kz + \overrightarrow{y}\sin kz] \qquad (1.33) \end{aligned}$$

In the basis where the quantization axis rotates so that it is always along the electric field and only π transitions are produced. Since the light shift is spatially uniform, this king of cooling cannot rely on Sisyphus effect. Nevertheless, the cooling derives from motion through a region of rotation of the quantization axis. Let us consider, once again, the simplest model, which is this time: $J_g = 1$ and $J_e = 2$. Moving atoms will experience a rotation of the quantization axis, and must be optically pumped in order to follow it. Hence, atoms traveling toward the σ^+ laser beam experience a large momentum change in the direction opposite to their motion, as $m_g = +1$ sublevel scatters six times more efficiently $\sigma^=$ than σ^- light[6], and as the atom remain

[6]Because of the Klebsh-Gordan coefficients

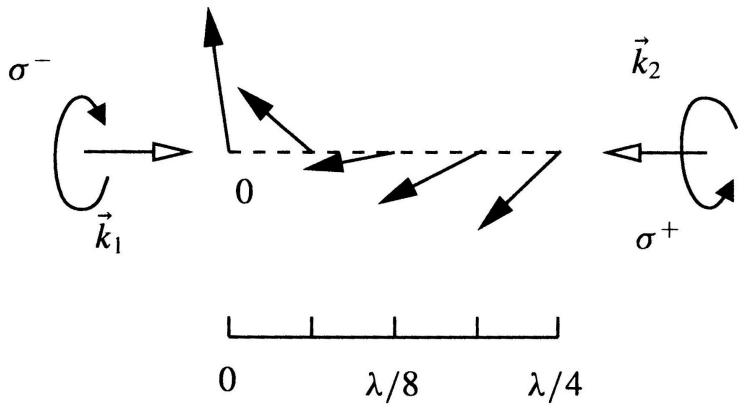

Figure 1.5: Polarization gradient field for the $\sigma^+ \perp \sigma^-$ polarization. Figure taken from [9]

in the $m_g = 1$ substate after an absorption/emission cycle. The same effect occurs in the other direction with σ^- beam and $m_g = -1$ substate. The atomic motion is damped by the differential scattering of light from the two laser beams.

1.2.4 The Magnetic Trap

The idea is that all the atoms with an angular momentum $\mathbf{F}$ have a magnetic moment $\mu = -\mu_B g_F \mathbf{F}$. Placed in a magnetic field of modulus $B(\mathbf{x})$, it precesses at the Larmor pulsation. If the latter is much greater than the characteristic frequency of the atom motion, the magnetic momentum follows adiabatically the field, with the potential energy $U(\mathbf{x}) = \mu_B g_F m_F B(\mathbf{x})$. As the magnetic field cannot have a maximum in the vacuum, the only way to get a potential minimum is to have the atom in a state such that: $g_F m_F > 0$. As $g_F < 0$ in the ground state, we will only catch the atoms in the $m_F = -1$ hyperfine state.

It is important to note that this part of the experiment only consists in trapping, not in cooling: the atoms will evolve following the potential described by the magnetic field, but they will not lose any energy.

Let us first describe the shape of the trap and the coils which create it (cf figure 1.6). The trap is axial (we will call z its axis), two sets of Helmoltz coils are along this axis: the smallest and the closest from the center of the trap are called *curvature coils* because they are responsible of the curvature of the field along the z axis; the others are called *anti-bias coils* because their main purpose is to compensate the field created in the center of the trap (called *bias field*) by the curvature coils, but without changing the curvature. The current flowing through the two sets of coils (called *main current*) comes in parallel from the same power supply, but go in opposite directions for the two sets, so that any noise of the power supply will not affect (too much) the bias field, because the effects on the coils will compensate each other. In order to control further the value of the bias field (B_0), an additional power supply runs current through the curvature coils, allowing thus to control the value of B_0 [7].

What about the radial magnetic field? The two sets of coils generate at the center of the trap a saddle point, which obviously is not the ideal shape for a trap! To compensate that effect, *gradient coils* are added. An easier case is showed on figure 1.7. The radial amplitude of B at

[7] Coming back to the MOT: for the Zeeman shift, we just needed a linear field as a function of the distance to the center of the trap. We just used one curvature coil, and the opposite anti-bias coil, running the same current trough these two coils, but in opposite directions.

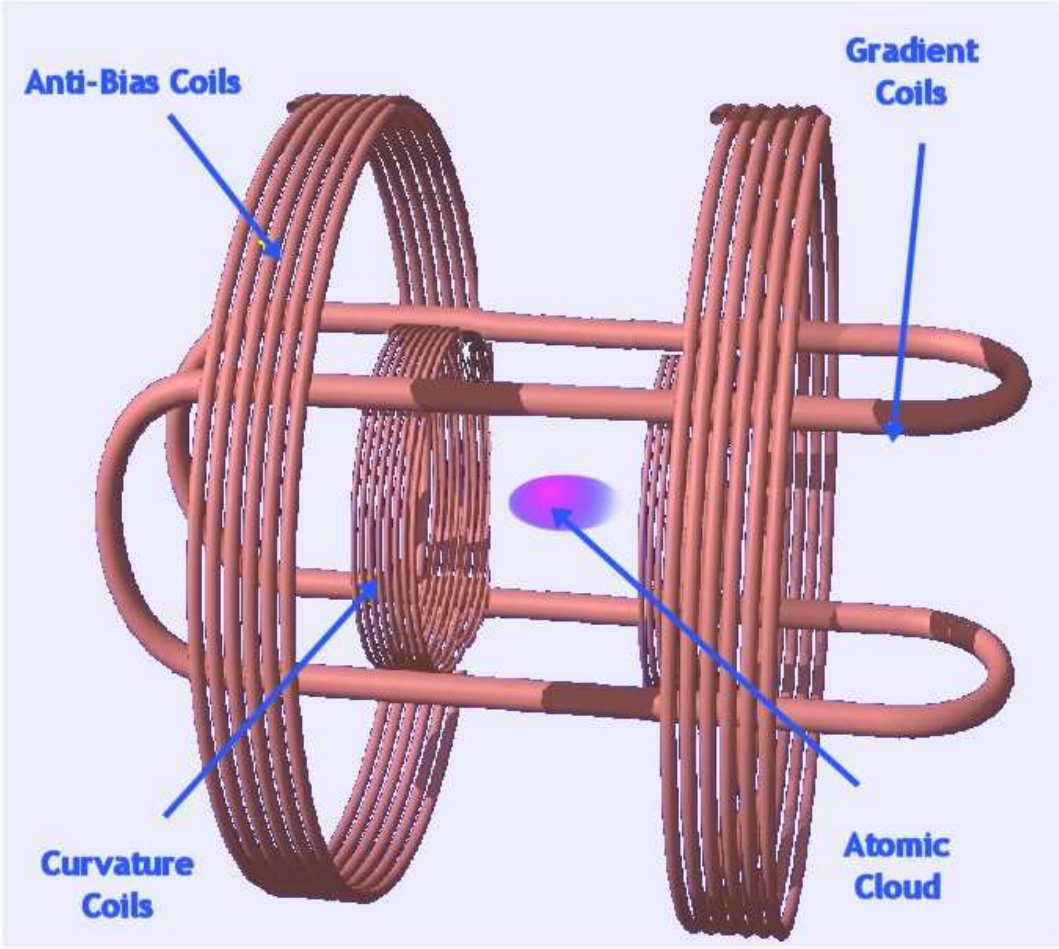

Figure 1.6: A Ioffe-Pritchard magnetic trap. Figure modified from [15]

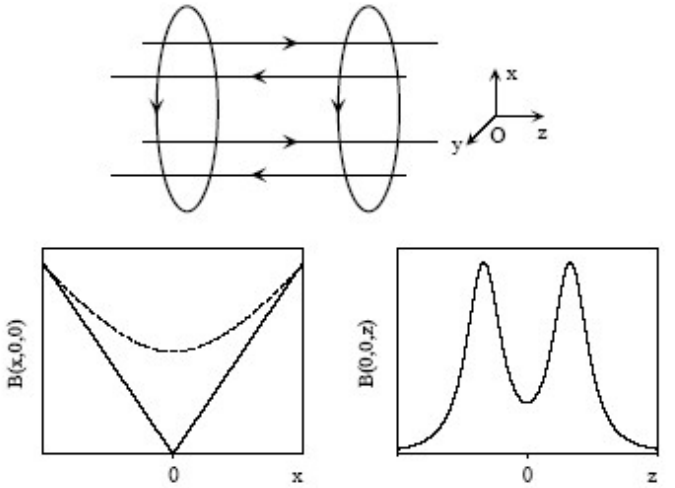

Figure 1.7: Ioffe configuration of the magnetic field. The curves represent the modulus of the magnetic field along the axis and in the transverse direction. In our case, an anti-bias et of coils has to be added, lowerig thus the field for $z = 0$. Figure taken from [3]

$z = 0$ is thus:

$$B(\rho) = \sqrt{B_0^2 + \rho^2 B'^2} = B_0 \sqrt{1 + \rho^2 \left(\frac{B'}{B_0}\right)^2} \simeq B_0 + \frac{1}{2}\frac{B'^2}{B_0}\rho^2 \tag{1.34}$$

The expression of B shows that the radial curvature of the field is given by B'^2/B_0. The most efficient way to get a cigare-shaped trap will thus be to decrease the bias field B_0 [8] The global magnetic field can be approximated by:

$$B(\rho, z) \simeq B_0 + B" z^2 + \frac{1}{2}\left(\frac{B'^2}{B_0} - \frac{B"}{2}\right) \tag{1.35}$$

How will practically be used this magnetic trap? Before turning on the current in the coils, the atoms must be in the ground state. There are mainly two ways of doing it: either by using a depumping laser[9], or by shutting the repump laser of the MOT a few ms before shutting off the MOT. The atoms will thus all be in the $F = 1$ state. Unfortunately, the atoms equally populate the $m_F = -1, 0, 1$ sublevels, and as our magnetic field will trap only $m_F = -1$ atoms, we are bound to loose 2/3 of the atomic cloud!
The coils are turned on. Typical values of the magnetic field are:

$$B_0 = 20\ G \tag{1.36}$$
$$B' = 85\ G/cm \tag{1.37}$$
$$B" = 25\ G/cm^2 \tag{1.38}$$

To get such magnetic fields, very high currents need to run into the coils (up to 600 A!). To prevent them from overheating, the coils are made of copper wires inside which high pressure water is run through[10].
The atomic cloud is first loaded into a spherical trap. Then it is slowly (in 3 s) curved. To do so, the main current is increased (to 400 A), the curvature current is decreased (from 400 A to 25 A) and the gradient current is increased (from 170 A to 300 A).

What is the point in creating a cigare-shaped cloud? There are mainly to assets: first, compressing the cloud will increase the collision rate and thus decrease the time needed for the system to thermalize; then it makes the detection of the BEC easier.

1.2.5 Evaporative Cooling

This is the last step to get a BEC. The idea is to get rid of the hottest atoms, so that after rethermalization, the cloud is colder. One can figure the motion of a trapped atom as an oscillation in the magnetic potential. The hottest atoms will be the one which climb the highest in the trap. They will thus experience the strongest Zeeman shift. A radio-frequency is broadcast through a coil in the vacuum chamber and will be absorbed by these atoms. They will switch from $|F = 1, m_F = 1 >$ to $|F = 1, m_F = 0 >$. In the latter state, atoms are not trapped any more. Hence, the hottest atoms are expelled from the trap starting from high radio-frequency ($\sim 30\ MHz$), and slowly sweeping down.

Provided the collision rate is sufficient to rapidly rethermalize the cloud, evaporative cooling should lead to BEC!

[8] However it is important not to cross the zero-field level, otherwise the shape of the magnetic field would be dramatically changed, with minima not out the center of the trap.

[9] The depumping is processed by using light which will send atoms from state $F = 2$ to $F' = 2$. They can either relax to $F = 2$ where they will once again be pumped to $F' = 2$, or to $F = 1$. Thus after a few ms, most of the population is in the $F = 1$ level.

[10] One of these wires was responsible for the leakage I mentionned earlier, leading to opening the vacuum chamber to fix it.

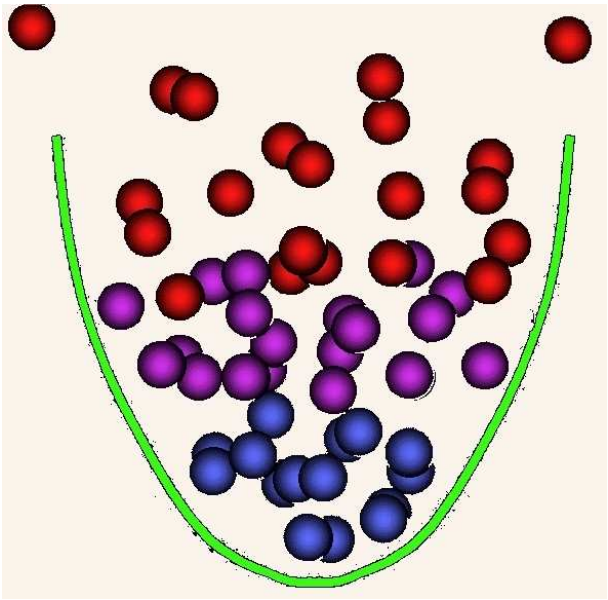

Figure 1.8: During the evaporative cooling, the depth of the magnetic trap is slowly decreased. The hottest atoms escape, and after rethermalization, the cloud is colder. Figure taken from [16]

1.2.6 State of our art

As I arrived in May, the first attempts to transfer atoms into the magnetic trap were achieved. The vacuum in the chamber was limited by a leakage at very high pressures (around 200 psi) in one of the water-cooled coils. First the water flow was inversed in hope the leakage was at a wire's end, but as the leakage persisted, the chamber was open, and the leakage fixed, by breezing the leaking coil to its input.The chamber was then baked during 10 days to go back to a high vacuum ($\sim 10^{-11}$ $Torr$). Appendix B briefly explains the different techniques to reach such vaccum conditions. Moreover the laser beams turned out to not to be well shaped and not to be powerful enough. A light amplifier was thus installed in order to get enough power. As the power was widely sufficient, the beam was filtered using a spatial filter and a monomode optical fiber. The outcoming beam was about 60 mW and had a correct shape.

These improvements lead to a 2 billion atom cloud in the MOT, and up to 600 million atoms in the magnetic trap. Some compression tests have been successfully tried. The collision rate increased during the compression but is not sufficient though.

The first attempts of evaporative cooling showed that the broadcast radio-frequencies were caught by almost all the electric appliances. The radio-frequencies were finally emitted from a coil inside the vacuum chamber. Requiring less power, it partly solved the problem.

A regime with higher collision rate has to be found to have the evaporative cooling work.

Chapter 2

The imaging system

We enter here more specifically into the work I achieved during these four months, and that I will finish in one month. My project was to set up an imaging system to take picture of the BEC, with different magnifications, and which could allow some quantitative measurement of it, such as temperature or density.

2.1 Different imaging techniques

This section is taken from [10].

Absorption, dark-ground and phase-contrast imaging Assuming the cloud is sufficiently thin so that light rays enter and exit the cloud at the same (x, y) coordinate[1] (this is the thin lens approximation), the complex electric field of the probe light after passage through the atomic cloud is:

$$\overrightarrow{E_0} \quad \longrightarrow \quad \overrightarrow{E}(x,y) = t.\overrightarrow{E_0} \exp i\Phi \tag{2.1}$$

Moreover, the optical density D, defined for resonant light as:

$$D(x,y) = \frac{\sigma_0}{1+\delta^2} \int n(x,y,z)\, dz, \tag{2.2}$$

where σ_0 is the resonant cross-section, $\delta = \frac{\omega-\omega_0}{\Gamma/2}$ the detuning and n the atomic density, can be related to the transmission t and the phase shift Φ [5]:

$$t = \exp -D/2 \tag{2.3}$$

$$\Phi = -\delta \frac{D}{2} \tag{2.4}$$

Thus by measuring either t or Φ, one can get the column density of the cloud $\tilde{n} = \int n(x,y,z)\, dz$.

This measures can be achieved by different ways:

Absorption image An absorption image is taken by shining a probe light through the sample, and then imaging the atomic cloud onto the camera. This gives a spatial image of the transmission $T = t^2$ of the cloud. This is the method we are currently using. As the laser beam is chosen resonant, the number of atoms in the sample can easily be derived:

$$N = \frac{A}{\sigma_0} \sum_{pixels} -ln(t^2(i,j)) \tag{2.5}$$

[1] The light is propagating along the z axis.

where A is the area imaged by a pixel.

Dark-ground image This image is taken by substracting the unscattered field to the electric field coming out of the cloud. This is achieved by placing a small dot in the center of the Fourier plan. Thus, the intensity on the camera can be written:

$$I_{dg} = \frac{1}{2}|E - E_0|^2 = I_0[1 + t^2 - 2t\cos\Phi] \tag{2.6}$$

Hence, for sufficiently low Φ, the signal is quadratic in ϕ.

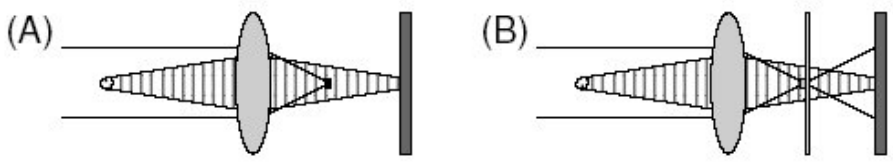

Figure 2.1: Darkground (A) and phase-contrast (B) imaging set-up. Probe light from the left is dispersively scattered by the atoms. In the Fourier plan of the lens, the unscattered light is filtered. In dark-ground imaging (A), the unscattered light is blocked, forming a dark-ground image on the camera. In the phase-contrast imaging (B), the unscattered light is shifted by a phase plate (consisting of an optical flat with a $\lambda/4$ bump or dimple at the center), causing it to interfere with the scattered light in the image plane. Figure taken from [5].

Phase-contrast image This technique is roughly the same as the latter, except that the black dot in the center of the Fourier plan is replaced by a $\lambda/4$ waveplate. The phase of the unscattered light is shifted by $\pi/2$. The intensity of a point in the image plane is then:

$$\begin{aligned} I_{pc} &= \frac{1}{2}\left|E + E_0\left(e^{i\frac{\pi}{2}} - 1\right)\right|^2 && (2.7)\\ &= I_0\left[t^2 + 2 - 2\sqrt{2}t\cos\left(\Phi + \frac{\pi}{4}\right)\right] && (2.8)\end{aligned}$$

which is linear in Φ.

***In situ* and time-of-flight imaging** We saw that the number of atoms in the cloud could be derived from the measure of the transmission. However, this method, called *In situ* imaging has its drawbacks: because the transmission drops exponentially with the optical density (i.e. with the column density), quantitative measurement requires the optical density to be on the order of 1. For typical condensates, $D \sim 300$ and thus, no quantitative information can be extracted from an absorption image.

Another method, called time-of-flight imaging, consists in turning off the magnetic trap so that the cloud expands and its density decreases, and take a picture after a variable time. This method is also very useful to measure the temperature of the condensate[2]. The shape of the expanding cloud after a very short time is depends on the shape of the trap, but after having expanded to a few times its original size, the shape of the clouds is a function distribution[3]. Hence, a measurement of the temperature can be derived.

[2]Indeed, at our stage of the experiment, this is the main use of time-of-flight imaging

[3]As the trajectory of the atoms can be considered as ballistic, which implies that the time between two collisions in the cloud is much bigger than the time of flight.

2.2 Realization of the imaging system

Our imaging system will require a probe laser enlightening the cloud in the top-bottom axis[4]. As this axis is also used by the MOT, there are only two solutions to avoid imaging the MOT light: either a beam-splitter is installed in the common path of the MOT and the probe lights and will split the beams, which should have different polarizations; or a flipper mirror is placed, and flips once the MOT light is shut down. As we would like to keep the polarization of the light for later work on spinor condensates, we chose the latter solution. On the other hand, we will not be able to take a picture of the MOT[5].

I will describe now what has been done to build this imaging system.

2.2.1 Setting up of the probe light

First, we need to get a laser beam at the right frequency. To do so, we take a part of an already existing beam by adding a $\lambda/4$ waveplate and a beamsplitter: the waveplate turns the polarization of the incoming light[6] of a given amount, and the cubic crystal sends the horizontal and the vertical polarizations in two orthogonal directions. We take the horizontal one for our probing purpose. As showed in figure **??**, we used the MOT laser light which was the closest from the transition we reached: $|F = 2> \rightarrow |F' = 3>$. The MOT laser is tuned 123 MHz under this transition. The modulation will be achieved using an Acousto-Optic Modulator (AOM). It is a small crystal in which a longitudinal acoustic wave is run trough a piezo-electric cell. Coming out are different orders of interaction of light with matter, giving rise to different frequencies: ω_l, $\omega_l \pm \omega_{ao}$, $\omega_l \pm 2\omega_{ao}$... The efficiency of a given order can be increased by modifying the angle between the incoming light and the crystal. AOMs are characterized by the frequency at which their efficiency is the best.

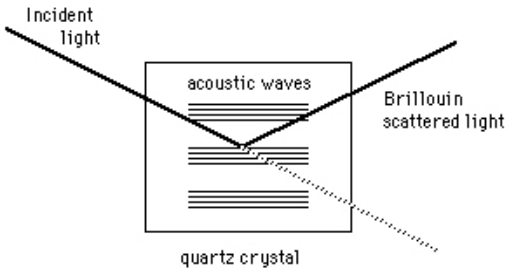

Figure 2.2: Light traveling through a quartz crystal can be diverted from its path by an acoustic wave. This process is called Brillouin scattering: from a classical point of view, the compression of the crystal will change the index of refraction, and therefore lead to reflection or scattering at any point where the index changes; from a quantum point of wiev, the process can be considered as the interaction of light photons with vibrational quanta (phonons). The modulation of the outgoing light is a function of the incident angle. Figure taken from [17]

I used a 80 MHz AOM to obtain the probe light. As the desired frequency at which I drove the crystal (123 MHz) was far from its optimum value, I got a bad efficiency (between 15 and 20%). But it did not really matter, as there was no need for high probing power.

[4]The windows of the top-bottom axis have better optical properties

[5]This drawback slowed dramatically down my work: as pictures of the MOT needed being taken to work on the 3 first steps of the experiments, I could work with the camera only when nobody else needed imaging the MOT! To take pictures of the MOT, another window was used, and the probe beam was sent to the cloud through another path.

[6]Most of the light on the table is vertically polarized

There is another way of setting an AOM called double pass. During my internship, I also set up the depumping beam (used before turning on the magnetic trap) using the double pass method. In the appendix C, I explain this method.

Once the right frequency is generated, probe light needs being mixed to the MOT light to be sent from the bottom to the top-bottom axis. This is achieved using a beamsplitter.

2.2.2 Setting up of the magnification system

After having crossed the atomic cloud, the probing light (which is now an absorption figure) exits the chamber through the top window. It goes then trough the magnification system. One would like to image the atomic cloud (or the BEC) at 1/2, 5 and 16 magnification. On that purpose a set of lenses and mirror was designed so that, depending on the position of the camera, the different magnification could be reached. Figure 2.3 shows the magnification system. There is an additional constraint: the polarization of the light must not be lost. This requires the use of gold mirrors, but it also restricts the number of mirrors that can be used. Currently, only classic mirrors are used, as we do not need to keep the polarization of the probe beam for the time being, and as gold mirrors are fragile.

In a first time, I tried to design the device on a single axis, but it was really difficult to do the alignment without any mirror. So I used the solution shown in figure 2.3.

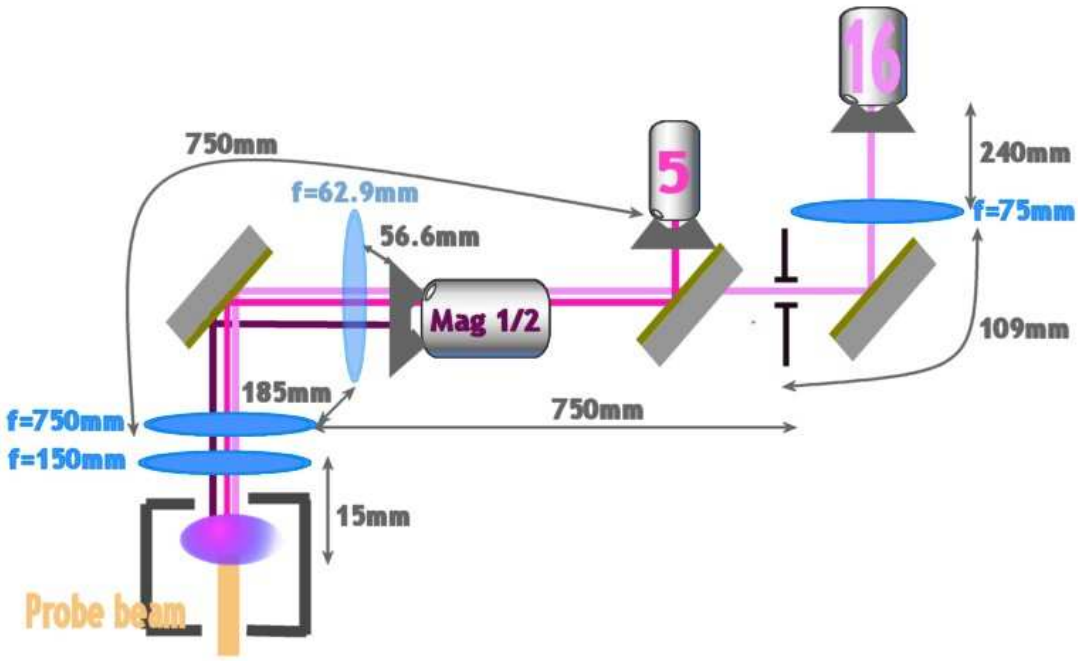

Figure 2.3: The imaging system and its 3 different magnifications.

In addition to the mirrors and lenses, some optics will ultimately be placed on the path of the beam:

- A mask in the path of the magnification 16. This mask hides a part of the chip on the camera, so that many shots in a row can be taken: a picture is taken on the enlightened part of the chip, then the picture is very quickly translated to other pixels of the chip and another picture can be taken on the enlightened part of the chip. Thanks to this method up to 30 pictures with a frequency of up to 1 kHz can be taken.

- Prisms which separate σ^+ and σ^- light. This prisms will be very useful to study spinor condensate: as different spin will absorb different polarizations, it will be interesting to take separate pictures of both polarizations.

2.3 Characterization of the imaging system

The difficult part of this work[7] is to characterize the system. This task is made difficult here because we do not exactly know neither the size of the atomic cloud, nor its shape. Thus it is very difficult to precisely focus on it and to know the magnification of the system. So here is the procedure I adopted: I first imaged the cloud with the 1/2 magnification. I focused it as well as I could. Then as one could not place any object in the center of the trap, I designed an optic path imaging on the camera a test pattern at the distance the atomic cloud should be of the camera. I set the position of the test pattern so that its image on the camera was well defined. Assuming that the camera focused well on the atomic cloud, I have now a very fine object virtually at the same position as the cloud. I can then do the same for magnification 5 and 16. The characterization device is represented in figure 2.4.

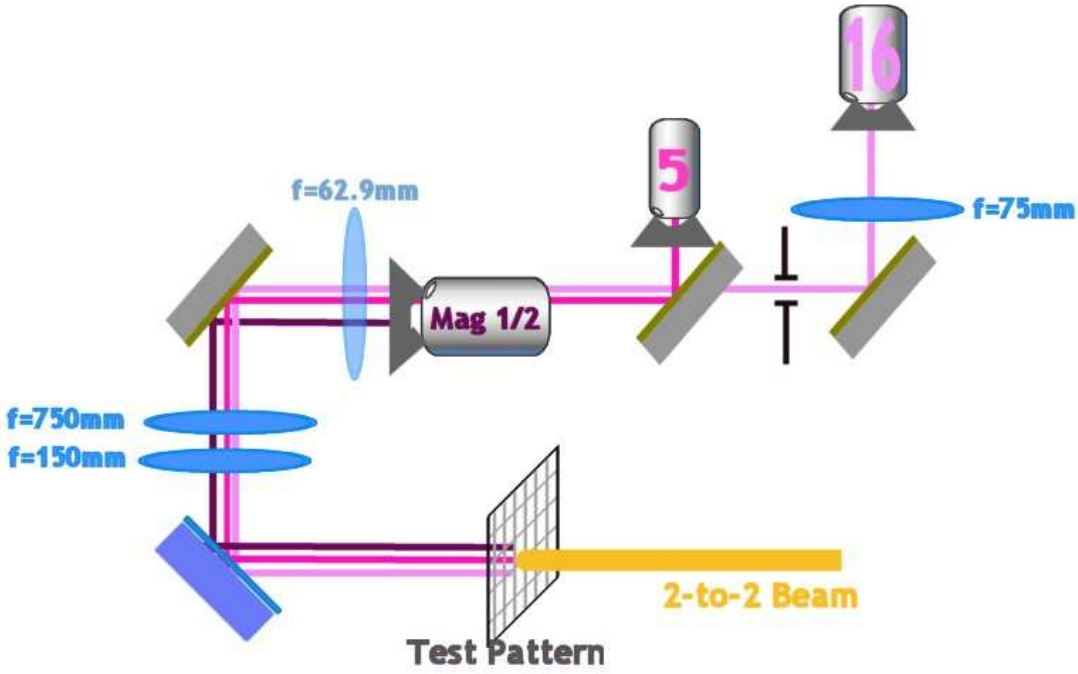

Figure 2.4: Placing a mirror between the cloud and the camera, and a test pattern in the object plan allows to determine the magnification of the system and gives an idea of the resolution of the system, as long as the mirror placed is not the smallest aperture of the system

Magnification 5 Let us start with this magnification because it is the easiest one: light only goes through two 2-inches lenses. The magnification measured with the test pattern is 4.56 ± 0.05. This is not exactly 5, but what really matters is the precision with which it is measured, because quantitative imaging relies on such value.

[7] If one excepts the problem of finding the room to install the system on an already crowded experiment!

The resolution will be determined by the smallest lines on the test pattern which can clearly be distinguished. It can be compared with a theoritical limit, assuming that the diffraction by the lenses is the limiting factor. To get an evaluation, the Rayleigh criterion for a lens is used:

$$d = 1.22\lambda F \tag{2.9}$$

where F is called F-number, and is the ratio of the focal lens over the clear aperture of the lens. In our case, as we have many lenses in a row, it is assumed that the diffraction is limited by the lens with the smallest F-number. It is important to notice that the value of the clear aperture is determined by the part of the lens which is effectively enlightened by the beam, and not by the real size of the lens. Figure 2.6 gives an example of how to determine the diffraction limit in the case of magnification 16. For magnification 5, the diffraction limit is evaluated: 3 μm.

The resolution measured is 9 μm. This is of the same order of magnitude, but does not exactly match the expected value. Three explanations can be given: first of all, the mirror has not been taken into account in our calculation because it is very difficult to tell which part is effectively enlightened, as the spot is not centered on it, it may thus be a limiting aperture; moreover, the approximation done in my calculation may be to strong, and we may have to do the exact computation; finally, the definition I give from the measured resolution may be wrong. Indeed, I am taking the distance between the *center* of the two smallest lines which can be distinguished. Using the distance between the closest edge would lead to a value of the resolution two times better.

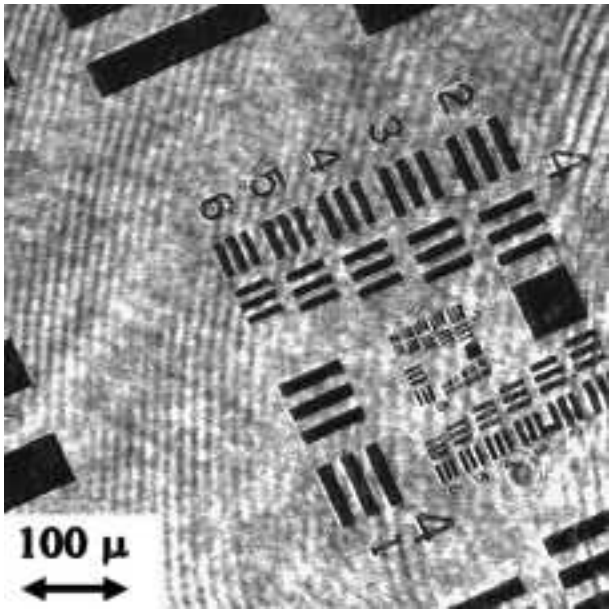

Figure 2.5: The test pattern imaged by the magnification 5 system. The smallest lines which can be distinguished are 4 μm-thick.

Magnification 1/2 For the magification 1/2, a 1-inch lens of 64 mm focal length is placed in the optical path. The magnification measured is 0.51 ± 0.02. The diffraction limit expected is roughly the same as before, as the lens added does not have the smallest F-number. However, the resolution measured is about 80 μm. This could be because, this size is close to the size of a pixel on the chip of the camera. Moreover, because of the shape of the lens, spherical aberrations have to be expected. It also creates distortion if slightly turned from its original position.

Magnification 16 For this magnification, a 1-inch, 75 mm lens is placed, leading to an expected diffraction limit of 12 μm. The magnification measured is 12.0 ± 0.5. The resolution measured is 20 μm. As for magnification 1/2, a slight rotation of the lens can lead to important distortions, but there is a greater problem: as the camera is moved forth and back, magnification significantly changes (about .35 magnification per cm), without changing the resolution. Thus, every time focusing is done on the cloud, many different positions of the camera can be found, with similar resolution, but very different magnification. It is then mandatory to remeasure the magnification of the system every time the focus is done.

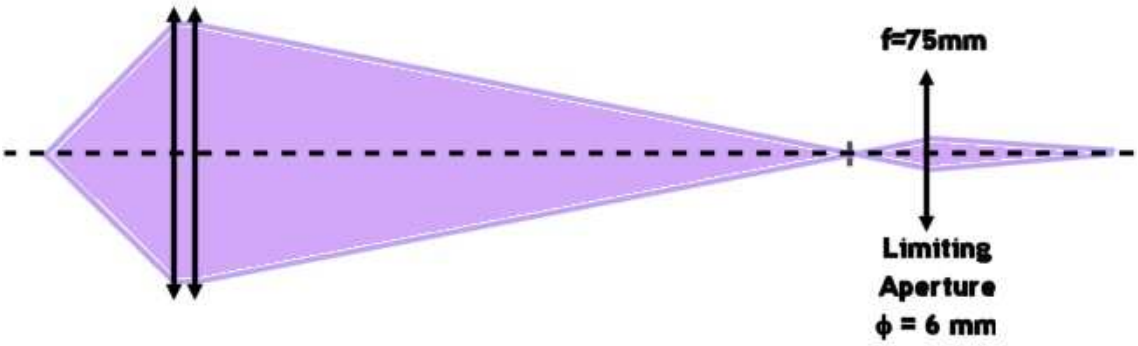

Figure 2.6: This is a schematic of how calculation of the diffraction limit is done: first the extremal paths, that is the paths which go from the cloud to the camera with the maximal deviation have to be found; then the biggest F-number have to be found, considering the effective aperture and the focal length of each lens. In the case of the magnification 16, the greatest F-number is for the last lens, giving a diffraction limit of 13 μm.

Conclusion The settings of magnification 5 seem satisfying. However, magnification 1/2 and 16 suffer from a high sensitivity to the position of the third lens. In the next month, different lens should be tried to solve that problem. Finally, as the magnification 16 changes significantly with the position of the camera, an easy way to fix and remove the mirror has to be found, so that the calibration of the system is made easier. That is the second axis I shall work on during the next month.

Chapter 3

WinView automation

The Roper Scientific's camera is controlled by a PC Software: `WinView`. With it, you can select the trigger mode, take pictures, do some basic image processing. The extensive use of images we do in this experiments urges us to automate the tasks as much as possible. On that purpose, `WinView` provides a macro editor. It is very easy to use (to write a macro, you just have to press a `Record` button and do the actions you want the macro to do; once finished, you just have to stop the record, `WinView` will automatically write the code), but not very reliable (there is no way to handle any error, which causes the macro to bug very often)!

There is another way to automate WinView, much heavier, but much faster and more powerful. This is the one I have been working on. It consists in writing add-ins for `WinView` in `Visual Basic`. Visual Basic is an object oriented language and Roper Scientific provides visual basic classes, allowing you to write procedures controlling `WinView`. Once written, you can transform these routines in buttons in `WinView`'s taskbar. In appendix, you will find the paper I write explaining how to translate the routines to buttons (or Snap-Ins). It is also important to note that this translation can only be achieved with `Visual Basic 6`[1].

In this section I will explain you the main features I added to `WinView`, and also the one I will probably write in the coming month...

3.1 The easiest ones: CloseAll, AutoSave and QuickASCII

CloseAll This function simply closes all the open windows. Though probably the easiest to write it is probably the most useful: indeed, every time you want to take an absorption image, you open 4 new windows (one containing all the shots, 2 corresponding to substractions of different shots, and the absorption image resulting of the division of the 2 later pictures). Before taking a new absorption image, you will be asked for each of the former windows if you want to close them!

As most of the time, you just want to close all the windows without saving them, the `CloseAll` button turns out to be very handy.

AutoSave Nevertheless, if you need to quickly save your images, `AutoSave` can be used. It takes all the pictures on the screen. It then determines wheter an image has to be saved or not: to do that the name of each image is read:

- If it is the default name for a picture taken by the camera, it will be saved as `RawData`.

[1] I spent 3 weeks trying to make it work on Visual Basic.NET, Microsoft's latest version of Visual Basic. With Visual Basic it took me 2 days to have my first add-in working!

- If it is called `Absorption`, it means that it is the result of a post-processing of the pictures taken of the cloud[2], and it will be saved as `Abs`
- Images named `pwa` or `pwoa` are just calculation steps in the post-processing leading to the absoprtion image. Thus they will not be saved.
- Files with any other name will be saved with their name unchanged.

Date and time are also automatically written on the name of the file. Finally, in order not to save twice the same pictures, files whose name finishes with a date and time will not be saved.

A former version displayed a list of all the open windows and you could select the one you wanted to save. By defaults all the pictures were selected. But this refinement was considered useless.

QuickASCII Finally, `QuickASCII` is a procedure which saves the image you are working on as a text file in which ach line contains the coordinates of a point, and its intensity. This allow you to process your data with `Igor` or `Matlab`.

3.2 Cycling absorption loop

In the frame of our experiment, the absorption imaging is the most used routine, as all the quantitative measurements (Temperature, number of atoms in the cloud, aspect ratio) are taken from the density column. Let us first describe the different steps of taking an absorption image:

- An acquisition is run during which four pictures are taken:
  - The first one cleans the captors of the CCD camera. It will not be used to get the absorption image, it is just a technical necessity.
  - Picture **2** contains the atomic cloud shone by the probe beam and the repump
  - Picture **3** contains the probe and the repump lights
  - Picture **4** only contains the repump light
- The background (i.e. picture **4**) is substracted to the pictures **2** and **3** so that the two new images are the one with only the probe light, and the one with the absorption of the probe light by the cloud[3].
- Getting the absorption image finally consists in dividing the image with the cloud by the image without: $\frac{\mathbf{2}-\mathbf{4}}{\mathbf{3}-\mathbf{4}}$

The whole process of creating the absorption image was achieved by a macro. The problem was that it was faulty: for example, if you decided to stop the acquisition before it was done, the program crashed. My first task was to write the Absorption routine in Visual Basic and to handle that kind of errors.

I then added a new feature: the Absorption routine can be cycled either a finite or infinite number of time, and each absorption can either be saved or overwritten. This option is of little interest currently but will probably be useful once a BEC is observed.

[2] This post-processing will be described in the next section

[3] These are the pictures which are automatically *not* saved by AutoSave: they only are a step in the calculation, there is no need to save them

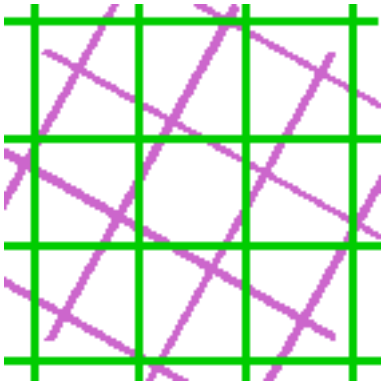

Figure 3.1: As the figure is represented by matrix, the coordinates of a pixel must be integer numbers. This is a problem for all the angles different from 90, 180 or 270 degrees.

3.3 Rotation of images

As the imaging system is not aligned with the magnetic field axis, it is very helpful to rotate the absorption images. For example it is easier to get the longitudinal and transverse shape of the atomic cloud: once turned transverse and longitudinal axis are along X and Y axis.

I tried four different rotation algorithms and found that the one using Cubic B-Spline interpolation was, by far, both the fastest and the nicest. I will review first the 3 different algorithms I implemented and then I will explain the B-Spline interpolation.

closest neighbor My first try used the easiest algorithm one could imagine: you take the coordinates of each pixel, you rotate them and you give the closest entire coordinate the value of the pixel. The rotated coordinates must be integers because they must correspond to the index of a matrix. The problem is that two pixels may have the same closest rotated neighbor, and thus some pixels could be overwritten, some information lost.

Gaussian interpolation I then tried to consider each pixel as a gaussian, centered on the index of the pixel, and of width 1 pixel. For each rotated pixel, I determined the 4 closest integer coordinates, I calculated the value of the gaussian for the four neighbors, I summed this four values to get a normalization factor. Finally each closest neighbor was given a part of the intensity of the rotated pixel weigthened by the value of the normalized gaussian. This method had one good asset: no intensity was lost in the rotation. On the other side, it was a bit slow (a few seconds), the rotated image lost in definition, and some periodic patterns sometimes appeared.

I varied the width of the gaussian to try to find a better compromise between the loss in definition and the regularity of the image, without changing the calculation time, but no significative improvement was found.

Cubic interpolation This method is much easier than the former. Each rotated pixel is shared between its 8 closest neighbors with fixed weightings:

0.0625	0.125	0.0625
0.125	0.250	0.125
0.0625	0.125	0.0625

Once again, no intensity is lost during the rotation, but the result is not convincing: a loss in resolution is observed, and some periodic patterns appear on the image.

B-Spline interpolation As said earlier, this rotation algorithm is much faster and give much better results than the ones I implemented first. It uses a technique developed by Michael Unser [11, 12, 13]. There are two main ideas:

- rather than trying to share the value of a rotated pixel between its closest neighbors, what if the discrete starting image was transformed into a continuous 2D graph $z(x, y)$? By that way, it would be easy to find the value of each pixel (i, j) in the final image, one would just do the inverse rotation and pick up the value of the *continuous* starting function: $I(i, j) = z[\Re^{-1}(i, j)]$. But a 2D high-quality interpolation requires high computation times...
- Hence the second idea, to split the rotation in three 1D transformations.

$$R(\theta) = \begin{bmatrix} \cos\theta & -\sin\theta \\ \sin\theta & \cos\theta \end{bmatrix} \tag{3.1}$$

$$= \begin{bmatrix} 1 & -\tan\frac{\theta}{2} \\ 0 & 1 \end{bmatrix} \begin{bmatrix} 1 & 0 \\ \sin\theta & 1 \end{bmatrix} \begin{bmatrix} 1 & -\tan\frac{\theta}{2} \\ 0 & 1 \end{bmatrix} \tag{3.2}$$

  By that way, we just need to interpolate line by line (or column by column) the image, which is far easier than a 2D-interpolation. This allows us to take a better interpolation, keeping affordable computation costs. There is also a way to transform the rotation into only two 1-D transformation, but as they rescale the image[4], it may add some noise to the rotation. That's why a 3-pass rotation will be implemented.

The interpolation will be achieved using B-Spline functions [1]: splines are piecewise polynomials. A B-Spline is a polynomial of fixed order, with a compact support and bell-shaped. "B" of "B-Spline" stands for "basis", as any Spline $s(x)$ of a given order n can be decomposed in the infinite summation of B-Spline β^n of this order:

$$s(x) = \sum_{k=-\infty}^{\infty} c(k)\beta^n(x-k) \tag{3.3}$$

A positive feature of B-Spline interpolation is called *local control*: if a point of the image is changed, only few coefficients will be affected thanks to the compact support of the B-Splines. Hence, an interpolation error will not spread on all the image.

My rotation algorithm will use cubic B-Spline because they give good results with fast calculations[5]:

$$\beta^3(x) = \begin{cases} 2/3 - |x|^2 + |x|^3/2 & 0 \le |x| \le 1 \\ 1/3 - |x|^3/6 & 1 \le |x| \le 2 \\ 0 & 2 \le |x| \end{cases} \tag{3.4}$$

The problem will be now to find the $c(k)$ coefficients which requires to invert $N \times N$ matrix based on eq. 3.3, where N is the length of a line (or a column) of the image (in our case, $N = 512$).

Let us use the z-transform to find a fast algorithm giving the coefficients $c(k)$. The z-transform of a discrete function $f_n$is defined by:

$$F(z) = \sum_{k=0}^{+\infty} f_n z^{-k} \tag{3.5}$$

[4]That is to say the determinant of each transformation is not 1

[5]I will not go further in the B-Spline theory: there are many different way to build the B-Splines, depending on the limit conditions that are chosen, hence there are many possible cubic B-Splines. M. Unser describes in detail the algorithm for a cubic b-spline interpolation [12]

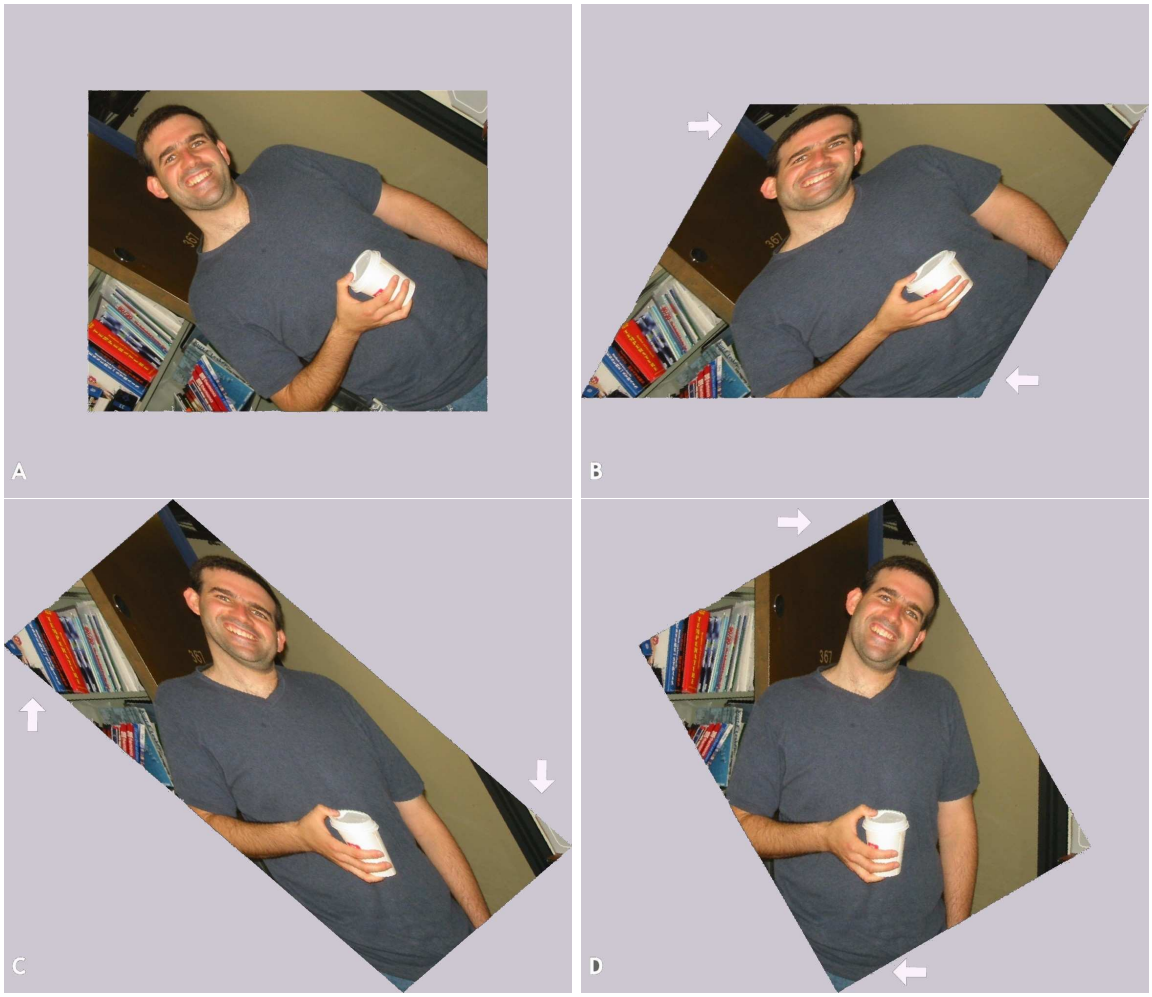

Figure 3.2: Illustration of the three-pass rotation algorithm: the original face (A) is first sheared along the x axis (B), then along the y axis (C), and finally once again along the x axis (D).

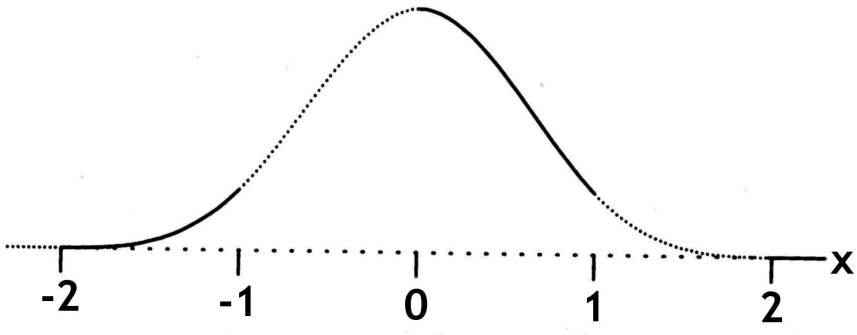

Figure 3.3: The uniform cubic B-Spline is a cubic C^2 basis function centered in 0. It is zero for $|x| \geq 2$. The nonzero portion is composed of four polynomial segments.

A straightforward demonstration would show that a convolution becomes a multiplication in the z-space and so:

$$s[k] = \beta^3 * c[k] \longleftrightarrow S(z) = B^3(z) \times C(z) \tag{3.6}$$

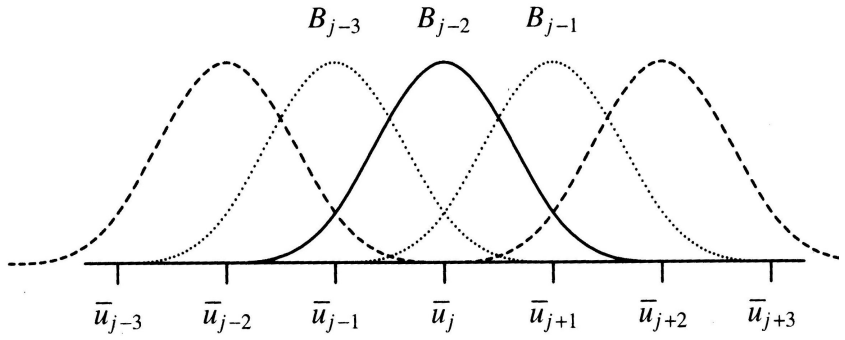

Figure 3.4: The basis functions that are not 0 at u_j are indicated by labels. Figure taken from [1].

Thus $c[k] \longleftrightarrow C(z) = (B^3)^{-1}(z) \times S(z)$ which means that we need to find $(B^3)^{-1}$, and take its inverse z-transform and convolve it by $s[k]$ to find $c[k]$

By sampling β^3 at the integers, we find that: $B^3(z) = \dfrac{z + 4z + z^{-1}}{6}$

Thus, the filter to implement is $(\beta^3)^{-1}(k) \longleftrightarrow \dfrac{1}{B^3} = \dfrac{6}{z + 4 + z^{-1}} = 6\left(\dfrac{1}{1 - z_1 z^{-1}}\right)\left(\dfrac{-z}{1 - z_1 z}\right)$

where $z_1 = -2 + \sqrt{3}$. In other words, the factorization of $1/B^3$ means that the convolution will be replaced by to easier ones. Using the "well-known" z-transforms:

$$a^n \longleftrightarrow \frac{z}{z - a} \tag{3.7}$$

$$a^{n-1} \longleftrightarrow \frac{1}{z - a}, \tag{3.8}$$

the convolutions are:

$$c^+[k] = \sum_{l=0}^{N-1} z_1^{k-l} s[l] \tag{3.9}$$

$$c[k] = \sum_{l=0}^{N-1} c^+[k - l]\left(\frac{1}{z_1}\right)^{k-1} \tag{3.10}$$

These two equations can finally be written in a recursive manner, and that is the way they will be implemented:

$$c^+[k] = s[k] + z_1 c^+(k - 1), \quad k = 1, ...N - 1 \tag{3.11}$$

$$c[k] = z_1(c[k + 1] - c^+[k]), \quad k = N - 2, ..., 0 \tag{3.12}$$

The limit conditions $c^+[0]$ and $c[N - 1]$ were given in the article, I took them as were.

Figures 3.5 and 3.6 show a comparison of all the rotation algorithms. The B-Spline is obviously by far the best method. All the more that the intensity of the pixels is conserved[6]

[6]This can be demonstrated by showing that the weighting factors generated by the cubic B-Spline function are normalized, i.e. for $0 \leq x < 1$, $\sum_k = -2^2\beta^3(x + k) = 1$

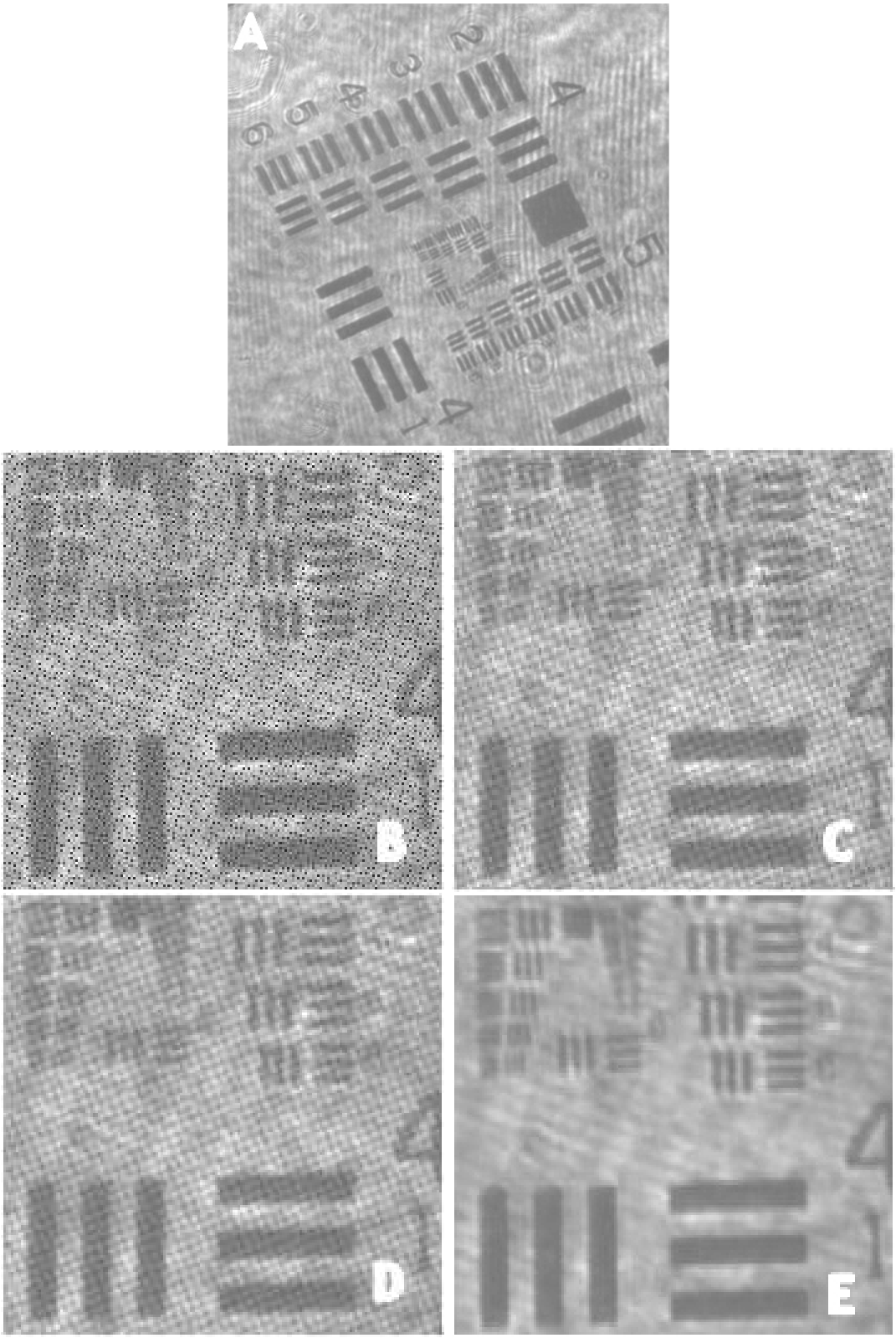

Figure 3.5: Comparison of the different rotation algorithms: (A) the original picure, (B) the closest neighbor, (C) the gaussian and (D) bicubic interpolations, (E) the B-Spline method. The closest method adds black points to the image, and the gaussian and bicubic method cause a decrease in resolution. B-Spline obviously gives the best results.

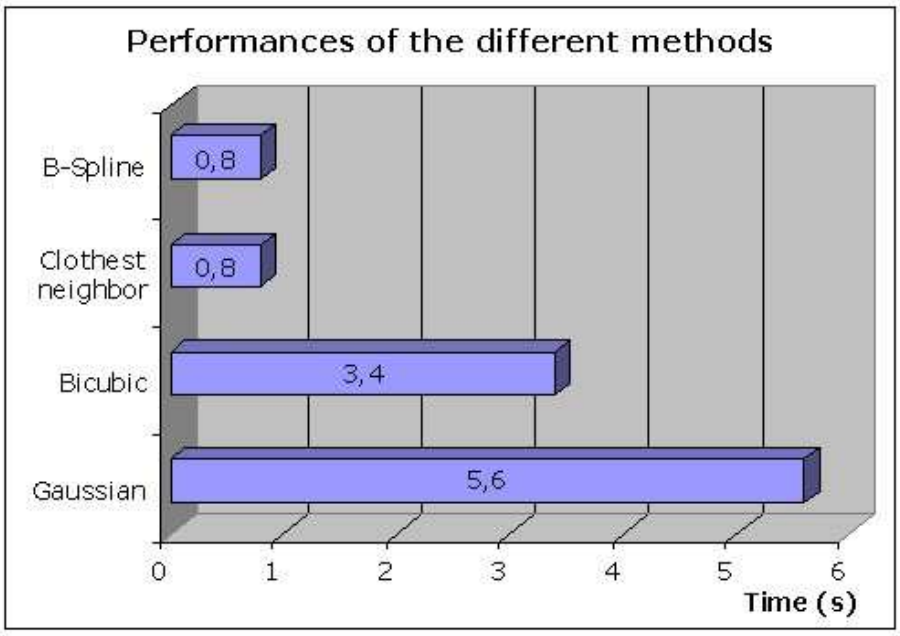

Figure 3.6: Times taken by the different methods for the rotations of figure 3.5

Conclusion

During the next month, I will work mainly on two tasks: finishing the imaging system, which consists in finding a way to make the calibration as easily reproducible as possible; adding a procedure to `WinView` to easily do a Gaussian fit of the profile of the cloud, and derive its temperature (the current method needs to save the data in ASCII and to read them with `Igor` which takes a lot of time for a very common measurement). The subsequent gain in time is very likely to give us a BEC sooner!

Such a short time for such a hugh experiment! Anyway, I learned a lot during this training period: about Bose-Einstein condensates of course, about experimental optics (I arrived knowing lenses and mirror, I will leave having understood almost every part of the experiment table, and being able to set most of it), about the amazing way American labs and universities work!

I would like to thank my supervisor Dan Stamper-Kurn for having hosted me in his young and dynamic team, to have had the force of getting through all the immigration hassle, and thanks to whom I had a really great time in California.

I would also like to warmly thank Lorraine and James for their patience and their numerous and excellent explanations. It was really a pleasure to work with them!

Appendix A: ^{87}Rb Spectroscopy

Rubidium is an alcalo-metallic atom, which means it has only one electron in its last occupied layer. Its atomic number is $Z = 37$, so that its electronic configuration is[7]: $[_{36}Kr]\ 5s^1\ 4d^0\ 5p\ 0$. Finally its atomic spin is $I = 3/2$.

These data should allow us to predict the spectroscopy of ^{87}Rb. For the ground state and the two first excited states, the fine structure due to spin-orbit coupling can be determined. In a second time, atomic and electronic spins will be coupled to give the hyperfine structure.

Coupling	Total Spin	Quantified values
$\overrightarrow{L}.\overrightarrow{S}$	$\overrightarrow{J} = \overrightarrow{L} + \overrightarrow{S}$	$\|L-S\| \leq J \leq L+S$
$\overrightarrow{I}.\overrightarrow{J}$	$\overrightarrow{F} = \overrightarrow{I} + \overrightarrow{J}$	$\|I-J\| \leq F \leq I+J$

A state will thus be characterized by its spectroscopic notation $^{2S+1}L_J$ and its total angular momentum F.

Remark: we are only interested in dipolar electric transitions. As the position operator is odd, we will only focus on the states of the opposite parity of the ground state. Thus the states arising from the $[Kr]\ 4d^1$ electronic configuration will not be taken into account, even if they are the first excited states, because the parity of the state is given by the parity of L, and it is the same as in the ground state.

Let us summarize the different states that are to be expected, ignoring the $[Kr]\ 4d^1$ electronic configuration:

Electronic configuration	$\overrightarrow{L}$	$\overrightarrow{S}$	Fine structure $\|L-S\| \leq J \leq L+S$	Spectroscopic notation	Hyperfine structure $\|I-J\| \leq F \leq I+J$
$[Kr]\ 5s^1$	0	1/2	1/2	$^2S_{1/2}$	$F=1$ $F=2$
$[Kr]\ 5p^1$	1	1/2	1/2	$^2P_{1/2}$	$F=1$ $F=2$
$[Kr]\ 5p^1$	1	1/2	3/2	$^2P_{3/2}$	$F=0$ $F=1$ $F=2$ $F=3$

Experimental measurements give the spectrum on the following figure .

About pumping... Most of our BEC experiments works with σ^+ polarized light, that is to say the optical transition will change the spin projection of the atom by $\delta m_F = +1$. Let us the $|F = 2 > \rightarrow |F' = 3 >$ transition, where $|F >$ and $|F' >$ are respectively the ground and

[7] The first unoccupied layers have been written here in order to find the first excited states of the atom

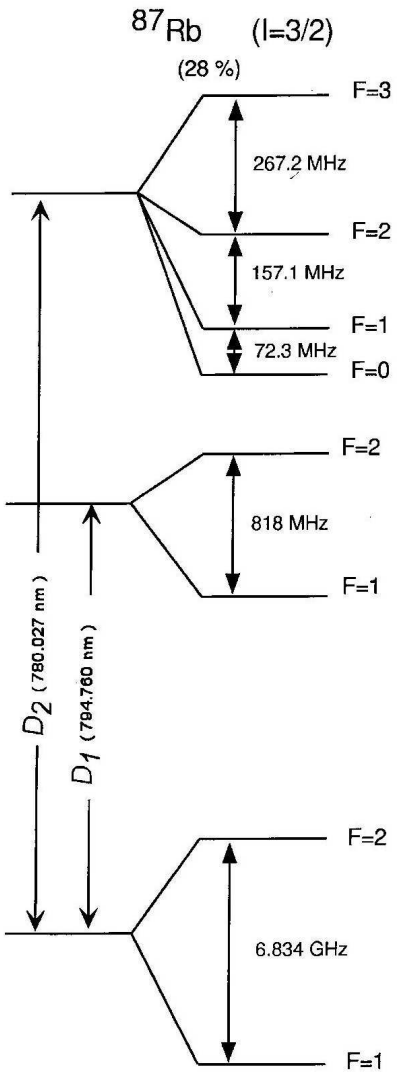

Figure 3.7: Fine and Hyperfine structure of ^{87}Rb for D_1 and D_2 transitions

the excited states: in absence of magnetic field, all the $|F, m_F>$ states for a given F have the same energy. Starting from any m_{F0} value, the atom will absorb a photon and be in a $|F', m_{F'} = m_{F0}+1>$ state. From their, the atom can be desexcited in 3 different ground states: $|F, m_F = m_{F0},\ m_{F0}+1,\ m_{F0}+2>$. This is imposed by the selection rules.

- If $m_F = m_{F0}$, the atom is back to its starting point
- Otherwise, the atoms has moved toward $|F = 2, m_F = 2>$ state.

After a few absorption/emission cycles, the atom is in the $|F = 2, m_F = 2>$ ground state. From their, with respect to the selection rules and to the polarization of the laser, the absorption/emission cycles will only occur between the $|F = 2, m_F = 2>$ and $|F' = 3, m_{F'} = 3$ states. Moreover, as the lifetime of the excited state is rather short ($\tau = 1/\Gamma \simeq 1/6\ Mhz \simeq 150\ ns$), the atoms are pretty quickly placed on the final transition.

In the presence of a Zeeman shift, things are much more complex, as the different m_F give different energy levels. Anyway the pumping laser will still be tuned on $|F, m_F = F>\rightarrow$

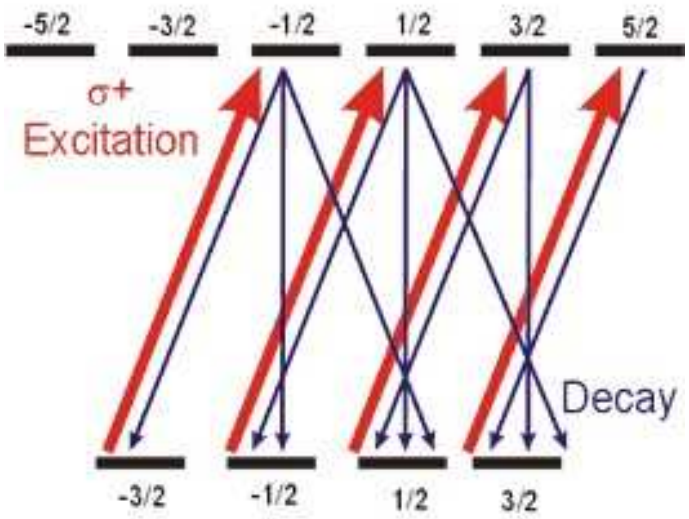

Figure 3.8: Principle of the optical pumping: the σ^+ light induces only $\Delta m = +1$ transitions, so that after a few absorption-emission cycles, the atom is in the $m = F$ state. Figure taken from [19]

$|F', m_F = F' >$. Atoms with $m_F \neq F$ will be far less efficiently pumped. But once they are on the $|F, m_F + F >$ state, only the $|F, m_F = F > \leftrightarrow |F', m_{F'} = F' >$ excitation/desexcitation path will be used, as the selection rules urge the excited state to relax into the $|F, m_F + F >$ state.

Appendix B: Vacuum techniques

The pressure below one atmosphere is loosely divided into vacuum categories [8]:

	Pressure ($Torr$)	Number Density (cm^{-3})	Mean free Path (cm)	Surface Collision Frequency ($cm^{-2}.s^{-1}$)	Times for Monolayer Formation (s)
One atmosphere	760	2.7×10^{19}	7×10^{-6}	3×10^{23}	3.3×10^{-9}
Lower limit of					
Rough vacuum	10^{-3}	3.5×10^{13}	5×10^{0}	4×10^{17}	2.5×10^{-3}
High vacuum	10^{-6}	3.5×10^{10}	5×10^{3}	4×10^{14}	2.5×10^{0}
Very high vacuum	10^{-9}	3.5×10^{7}	5×10^{6}	4×10^{11}	2.5×10^{3}
Ultrahigh vacuum	0				

Reaching Ultrahigh vacuum

Vacuum pumps operate in a limited pressure range. In general, a pump that operates in the viscous flow will not operate in the molecular flow and vice versa. Going from 10^3 down to 10^{-11} $Torr$ will require at least two different pumps.

Oil-sealed rotary pump This one is the most commonly used for attaining pressures down to a few $mTorr$. A rotor turns off-center within a cylindrical stator. The interior of the pump is divided into two volumes by an ellipsoidal piece attached to the rotor. Gas from the pump inlet enters one of these volumes and is compressed and forced to the exhaust. The seal between the stator and the edge of the cylinder is maintained by a thin film of oil.

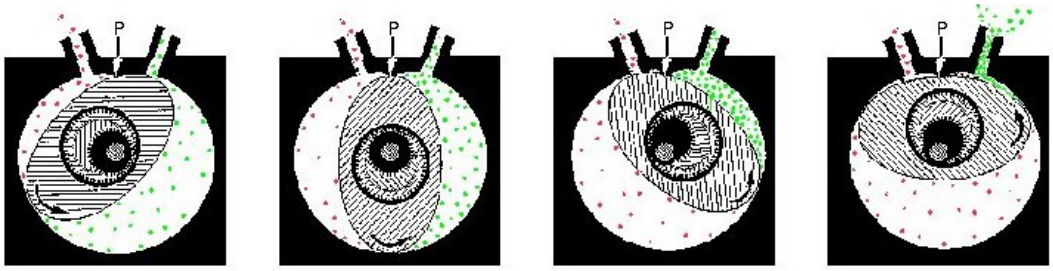

Figure 3.9: Decomposition of a cycle of a rotary pump. Figure taken from [18]

Turbomolecular pump Below 10 $mTorr$, the turbomolecular pump is turned on. Nevertheless, the rotary pump keeps on pumping the outlet of the turbomolecular pump, we will see why. In this pump, a bladed turbine rotor turns at $70,000$ rpm. The edge speed of the rotor

approaches moecular velocities. When a molecule strikes a rotor blade, a significant component of velocity in the direction of the pump exhaust is transferred to the molecule (see figure 3.10). These pumps provide roughly the same pumping speed for all gases; however, the compression ratio (i.e. the ratio of outlet to inlet pressure) depends upon the nature of the gas being pumped. This ratio increases with the molecular weight. For example, a pump with a compression ratio of 10^7 for N_2 will have a compression ratio of only 10^2 for H_2. An explanation could be that light particles cross more easily the rotor in both sens. Consequently, the compression ratio is very high for oil vapor backstreaming from the rotary pump. Thus a turbopump provides an essentially oil-free vacuum.

The compression ratio is also extremely sensitive to the pressure at the outlet of the turbopump. A typical pump will have a compression ratio of 10^7 for air if the pressure at the exhaust is .1 $Torr$, but if the exhaust pressure rises to 1 $Torr$, the ratio falls to 10. Hence the interest of running the turbopump in series with the rotary pump.

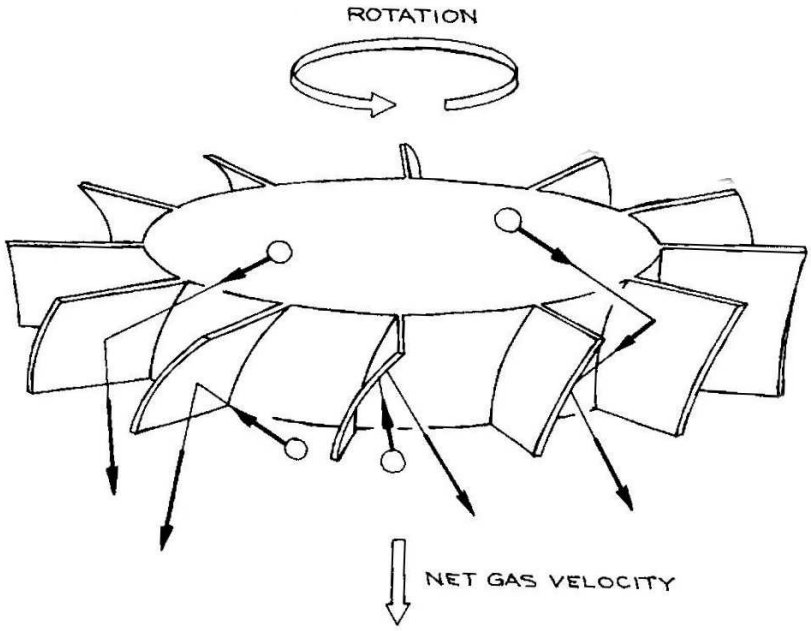

Figure 3.10: Rotor of a turbomolecular pump. Figure taken from [8]

With the two previously mentionned pumps, 10^{-7} $Torr$ is reached. To pump further a baking of the chamber is required.

Bake-out With the two previously mentionned pumps, 10^{-7} $Torr$ is reached. To achieve pressures much below 10^{-7} $Torr$, baking is required in order to remove water and hydrocarbons from vacuum-system walls. Heating to $50 - 100^oC$ for several hours improves the ultimate presssure of most systems by an order of magnitude. In our case, the chamber was baked during 10 days: the temperature was progressively increased from 90^oC up to 200^oC. The composition of the vacuum was monitored by a RGA-spectrometer (for Rare Gas Analyzer). The partial pressures slowly dropped. When a plateau was reached, the temperature was increased to desorb further the particles. Once the baking finished and the vacuum chamber back to room temperature, the pressure was below the threshold of the gauge, i.e. 10^{-10} $Torr$.

Keeping Ultrahigh vacuum

As our experiment is very sensitive to vibrations, turbomolecular pump cannot be run all the time. Once ultrahigh vacuum is attained, two other pumps are used, and the turbopump is turned off.

Ion pump A magnetically confined discharge is maintained between an anode and a Titanium cathode. The discharge is initiated by field emission when a potential of about 7 kv is placed across the electrodes. After the discharge is struck, the rate is maintained by a power supply. Inert gas molecules, and other molecules as well, are ionized in the discharge and acceleretad into the cathode with sufficient kinetic energy that they are permanently buried. Active gases are chemisorbed by Titanium thas has been sputtered off the cathode by ion bombardment and deposited on the anode.

Titanium sublimation pump In this pump, the active metal surface is produced *in vacuo*. Titanium wires are wrapped around a Tungstene heater filament contained surrounded by walls cooled with liquid Nitrogen. This filament is electrically heated to evaporate the Titanium, which condenses on the walls. Below 10^{-7} $Torr$, the Titanium only need be deposited periodically. Figure 3.11 shows such a simple titanium sublimation pump, that is the bulb is not nitrogen cooled, contrary to the pump we use.

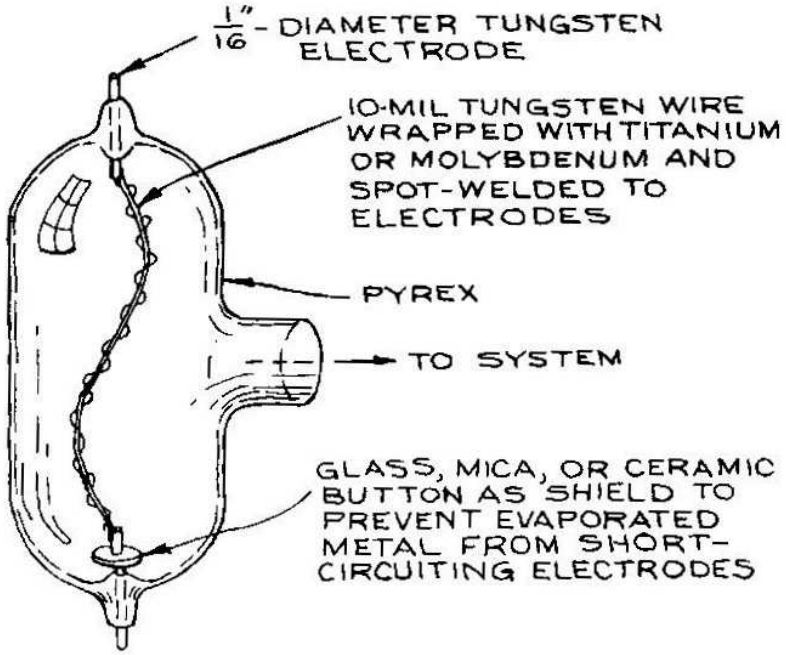

Figure 3.11: Simple Titanium sublimation pump. Figure taken from [8]

Appendix C: double-pass AOM

This technique shifts a laser beam of twice the AOM frequency. The send the light forth and back into the AOM, so that each path leads to increase (or decrease) the frequency of ω_{ao}.

Figure 3.12 shows the experimental device: the laser light first goes through a convex lens to gently focus the beam on the AOM, so that all the beams are almost parallel (the typical focal lens is 400 mm). The light has to be either vertically or horizontally polarized. It will cross a beam-splitter whom utility will appear later. It goes then into the AOM, and the light of the desired order comes out with a small deviation. The AOM is placed in the object plan of a lens, so that all the orders are parallel after the lens. A $\lambda/4$ waveplate transforms the linear into a circular polarization. An iris selects the desired order. Eventually a mirror is placed, perfectly orthogonal to the beam.

The light takes thus the reverse way: crossing again the waveplate, its polarization is now orthogonal to its original one; it focuses then on the AOM, comes out right in the axis of the incoming light[8], and the beam-splitter sends the light into an orthogonal direction.

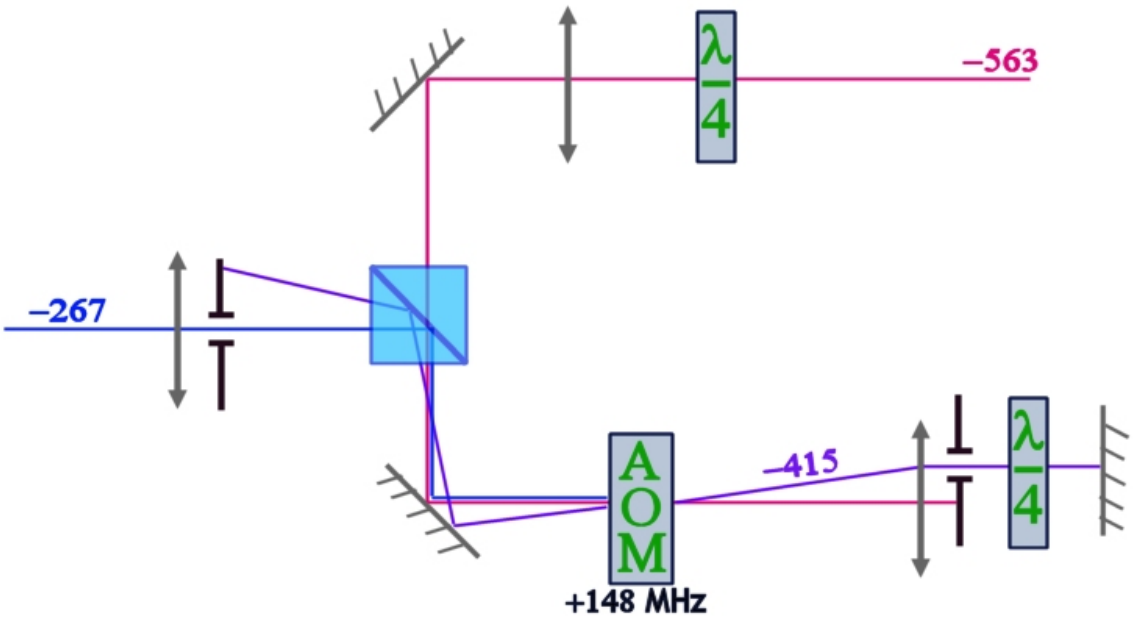

Figure 3.12: Double-pass AOM settings for the 2-to-2 beam. All the lenses are focused on the AOM, so that the light coming and out from the system is parallel. The incoming laser frequency is 523 MHz under the 2-to-3 transition.

My double-pass AOM was designed for the $|F = 2 > \rightarrow |F' = 2 >$ transition, also called

[8]Indeed, the light is deviated from θ during the way forth. On the way back, it enters the AOM with the angle $-\theta$, and the frequency shift, once again, deviates the light of θ. Eventually the light comes out with a deviation of $-\theta + \theta = 0$.

"2-to-2 beam". It had to be tuned 267 Mhz below the 2-to-3 beam (cf. figure 3.7). The light was taken from the slower beam which is 563 MHz red-detuned and doubled-passed through a 200 MHz driven by a 148 MHz sinusoidal current of 1.1 W.

The incoming light was 2.08 mW. After the first pass, the power of the beam was 1.40 mW, and 1.00 mW after the second one. The efficiency is thus $\underline{\rho = 48\%}$. The efficiencies of the first and second pass are different because in the first pass, a part of the light was lost because it did not go through the window of the AOM, which was not the case in the second pass.

Appendix D: The art of making add-ins for WinView in Visual Basic 6

Appendix E: Code of RotateDefault

In order to save trees, only the code for the `RotateDefault` program is reported here, as it is probably the most relevant. The other are available on the web:
http://www.ens-lyon.fr/ flienhar/BEC/index.html

In this case, an Add-In was created using the protocol describe in the Appendix D, and only the `PISnapIn_OnCommand` of the `clsSnapIn` class was modified and a few subroutine were added to the same class. Hence only these subroutines from the `clsSnapIn` class are written here:

```
Public Sub PISnapIn_OnCommand(ByVal lpUnk As Object)
    ' This code is executed when the user in WinX/32 depresses
' the toolbar button or selects the menu item associated with this snap-in
    ' The rotation value will be read in a text file placed in the default folder,
    ' that is where all the WinView files are saved...
    If Windz.Count = 0 Then
        WinX.StatusBarMsg 0, 0, "No image to work on!"
    Else
        Set WindOld = Windz.GetActive()
        Set DocOld = WindOld.GetDocument()
        'Gets the angle value
            Dim FileHandle%
            Dim strDFNFull As String, strDFNLeft As String, strPath As String
            Dim intSlash As Integer
            Dim strBuff As String, strText As String
            Dim Alpha As Double
            ' Get the default location of the saved data
            strDFNFull = ExpVB.GetParam(EXP_CMD.EXP_DATFILENAME)
            intSlash = InStrRev(strDFNFull, "\")
            strDFNLeft = Left(strDFNFull, intSlash - 1)
            strPath = strDFNLeft & "\DefaultAngle.txt"
            'Get a free file handle and assign it to the file handle variable
            FileHandle% = FreeFile
            Open strPath For Input As #FileHandle% 'Open the file
            'Traverse the lines of the file
            Do While Not EOF(FileHandle%) 'Check for end of file
                Line Input #FileHandle%, strBuff 'Read a line of the file
                strText = strText & strBuff 'Add the line from the output buffer
            Loop
            If Not IsNumeric(strText) Then
                MsgBox "The default angle is not a number. You can change it " & _
                        in the " & strPath & " file. Meanwhile, rotation was " & _
                        "set to 45.", vbOKOnly, "Wrong argument value"
```

```
                strText = 45
            End If
            Close #FileHandle% 'Close the file when completed
        ' Check if the image canbe treated by the RotateSpline routine
        If strText > 90 Or strText < -90 Then
            MsgBox "The default angle is not between -90 and 90. You can change " & _
                   "it in the " & strPath & " file.", vbOKOnly, "Out of range"
            Exit Sub
        End If
        If DocOld.GetParam(DM_XDIM) > 512 Or _
            DocOld.GetParam(DM_YDIM) > 512 Then
            MsgBox "Spline method can only handle images smaller than 512x512. " & _
                   "Sorry!", vbOKOnly, "Format mismatch"
            Exit Sub
        End If
        RotateSpline CDbl(strText)
    End If
End Sub

Private Sub RotateSpline(Alpha As Double)
    'RotateSpline is a powerfull rotation algorithm. The rotation is
    'splitted in 3 1D transformation of det=1. So that each line can be
    'considered as a 1D signal, and thus can be easily interpolated.
    ' The interpolation is a cubic-spline one.

    Dim array1(0 To 514, 0 To 517) As Double
    Dim array2(0 To 1028, 0 To 517) As Double
    Dim array3(0 To 1028, 0 To 750) As Double

    'Selects the image to rotate and puts it in frOld
    Dim Curse As New CursorObj
    Set Curse = WindOld.GetCursor
    DocOld.GetFrame Curse.ZPos, frOld

    'Creates the new frame
    strMethod = " Spline"
    strShortMethod = "S"
    Inf.x = 750
    Inf.Y = 750
    Inf.Z = 1
    Inf.dataType = DocOld.GetParam(DM_DATATYPE)
    Inf.Name = "Rotation " & Round(Alpha) & strMethod
    Inf.FileType = dt_SPE
    DocNew.OpenNew "", Inf
    DocNew.GetFrame 1, frNew
    'White background
    Dim intA As Integer, intB As Integer
    For intA = 0 To 749
        For intB = 0 To 749
```

```
            frNew(intA, intB) = 1
        Next intB
    Next intA

    'Writes the rotation informations in the comments
    DocNew.SetParam DM_USERCOMMENT1, "Rotation"
    DocNew.SetParam DM_USERCOMMENT2, Alpha
    DocNew.SetParam DM_USERCOMMENT3, DocOld.GetParam(DM_XDIM)
    DocNew.SetParam DM_USERCOMMENT4, DocOld.GetParam(DM_YDIM)
    DocNew.SetParam DM_USERCOMMENT5, strShortMethod

    'Copies the image at the right position: array is bigger than frOld.
    ' Thus, out of range problems are avoided
    Dim kx As Integer, ky As Integer
    Dim offsetX As Integer, offSetY As Integer
    Dim oldDimX As Integer, oldDimY As Integer
    oldDimX = DocOld.GetParam(DM_XDIM)
    oldDimY = DocOld.GetParam(DM_YDIM)
    offsetX = Ent((512 - oldDimX) / 2)
    offSetY = Ent((512 - oldDimY) / 2)

    For kx = 0 To oldDimX - 1
        For ky = 0 To oldDimY - 1
            array1(offsetX + kx, offSetY + ky) = frOld(kx, ky)
        Next ky
    Next kx

    ' Sets the following values
    Dim si As Double, ta2 As Double, dcoef As Double, a As Double
    si = Sin(Alpha / 180 * 3.14159)
    ta2 = Tan(Alpha / 360 * 3.14159)
    dcoef = 100 / 1533 'for the progress bar
    a = -2 + Sqr(3) 'for the convolution which gives the interpolation function

    'Rotates the Image
    Dim k As Integer
    Dim cs1 As Double, cs2 As Double, cs3 As Double, cs4 As Double ' weighting function
    Dim cplus(0 To 1028) As Double
    Dim cminus(0 To 1028) As Double
    Dim dSum As Double
    Dim decPart As Double, intPart As Integer, dFirst As Double
    Dim intMin As Integer, intMax As Integer

''''''''''''''''''1st Pass''''''''''''''''''''''''''
    For ky = 0 To 511
        ShowProgress ky * dcoef
        'Interpolation computation
            '1. End condition cplus(0)
            dSum = 0
```

```
            For k = 0 To 5
                dSum = dSum + a ^ k * array1(k, ky)
            Next k
            cplus(0) = dSum
            '2. Calculation of c+
            For k = 1 To 514
                cplus(k) = array1(k, ky) + a * cplus(k - 1)
            Next k
            '3. End condition of cminus(N-1)
            cminus(514) = a / (1 - a ^ 2) * (cplus(514) - a * cplus(513))
            '4. Calculation of c-
            For k = 513 To 0 Step -1
                cminus(k) = a * (cminus(k + 1) - cplus(k))
            Next k

            'Calculates the weighting coefficients
            dFirst = 256 - ta2 * (ky - 256)
            intPart = Ent(dFirst)
            decPart = (dFirst) - intPart
            cs1 = cubSpline1(decPart)
            cs2 = cubSpline2(decPart + 1)
            cs3 = cubSpline3(decPart + 2)
            cs4 = cubSpline4(decPart + 3)

            For kx = 0 To 511 'Shearing
                array2(intPart + kx, ky + 3) _
                                    = cs1 * array1(kx, ky) _
                                    + cs2 * array1(kx + 1, ky) _
                                    + cs3 * array1(kx + 2, ky) _
                                    + cs4 * array1(kx + 3, ky)
            Next kx
        Next ky

''''''''''''''''''2nd Pass''''''''''''''''''''''''''
    Dim width As Integer
    width = Round(514 * (1 + Abs(ta2))) 'Width of the sheared window
    offsetX = Ent((1028 - width) / 2) 'Absiss of the 1st point of the sheared picture
    dcoef = 100 / (width - 1) / 3
    For kx = offsetX To offsetX + width - 1
        ShowProgress 33 + (kx - offsetX) * dcoef

        ' Gets the extreme plotted points of the tx-th column
            intMin = 0
            Do While array2(kx, intMin) = 0 And intMin < 511
                intMin = intMin + 1
            Loop
            intMin = intMin - 3
            intMax = 511
            Do While array2(kx, intMax) = 0 And intMax > 0
```

```
            intMax = intMax - 1
        Loop
        intMax = intMax + 3

    'Interpolation computation
        '1. End condition cplus(0)
        dSum = 0
        For k = intMin To intMin + 5
            dSum = dSum + a ^ k * array2(kx, k)
        Next k
        cplus(intMin) = dSum
        '2. Calculation of c+
        For k = intMin + 1 To intMax
            cplus(k) = array2(kx, k) + a * cplus(k - 1)
        Next k
        '3. End condition of cminus(N-1)
        cminus(intMax) = a / (1 - a ^ 2) * (cplus(intMax) - a * cplus(intMax - 1))
        '4. Calculation of c-
        For k = intMax - 1 To intMin Step -1
            cminus(k) = a * (cminus(k + 1) - cplus(k))
        Next k

    'Calculates the weighting coefficients
        dFirst = 117 + si * (kx - 512) '119=379-256 : 1st point of the kx-th column
        intPart = Ent(dFirst)
        decPart = (dFirst) - intPart
        cs1 = cubSpline1(decPart)
        cs2 = cubSpline2(decPart + 1)
        cs3 = cubSpline3(decPart + 2)
        cs4 = cubSpline4(decPart + 3)

    'Shearing loop
        For ky = intMin To intMax
            array3(kx, intPart + ky) _
                                = cs1 * array2(kx, ky) _
                                + cs2 * array2(kx, ky + 1) _
                                + cs3 * array2(kx, ky + 2) _
                                + cs4 * array2(kx, ky + 3)
        Next ky
    Next kx

''''''''''''''''''3rd Pass''''''''''''''''''''''''
 Dim height As Integer
 height = Round(514 * (1 + Abs(si) * (1 - Abs(ta2))))
 offSetY = Ent((750 - height) / 2)
 dcoef = 100 / (height - 1) / 3
 For ky = offSetY To offSetY + height - 1
     ShowProgress 67 + (ky - offSetY) * dcoef
```

```
        ' Gets the extreme plotted points of the tx-th column
            intMin = offsetX
            Do While array3(intMin, ky) = 0 And intMin < offsetX + width - 5
                intMin = intMin + 1
            Loop
            intMin = intMin - 3
            intMax = offsetX + width
            Do While array3(intMax, ky) = 0 And intMax > offsetX + 3
                intMax = intMax - 1
            Loop
            intMax = intMax + 3

        'Interpolation computation
            '1. End condition cplus(0)
            dSum = 0
            For k = intMin To intMin + 5
                dSum = dSum + a ^ k * array3(k, ky)
            Next k
            cplus(intMin) = dSum
            '2. Calculation of c+
            For k = intMin + 1 To intMax
                cplus(k) = array3(k, ky) + a * cplus(k - 1)
            Next k
            '3. End condition of cminus(N-1)
            cminus(intMax) = a / (1 - a ^ 2) * (cplus(intMax) - a * cplus(intMax - 1))
            '4. Calculation of c-
            For k = intMax - 1 To intMin Step -1
                cminus(k) = a * (cminus(k + 1) - cplus(k))
            Next k

            'Calculates the weighting coefficients
            dFirst = -137 - ta2 * (ky - 375) '-139=375-514
            intPart = Ent(dFirst)
            decPart = (dFirst) - intPart
            cs1 = cubSpline1(decPart)
            cs2 = cubSpline2(decPart + 1)
            cs3 = cubSpline3(decPart + 2)
            cs4 = cubSpline4(decPart + 3)

            For kx = intMin To intMax 'Shearing
                frNew(intPart + kx, ky) _
                                    = cs1 * array3(kx, ky) _
                                    + cs2 * array3(kx, ky + 1) _
                                    + cs3 * array3(kx, ky + 2) _
                                    + cs4 * array3(kx, ky + 3)
            Next kx
        Next ky
    DocNew.PutFrame 1, frNew
    DocNew.Update
```

```
    WinX.StatusBarMsg 0, 0, "Rotation completed"
    ShowProgress 0
End Sub

Private Function cubSpline1(x As Double) As Double
    cubSpline1 = x ^ 3 / 6
End Function

Private Function cubSpline2(x As Double) As Double
    cubSpline2 = -(3 * x ^ 3 - 12 * x ^ 2 + 12 * x - 4) / 6
End Function

Private Function cubSpline3(x As Double) As Double
    cubSpline3 = (3 * x ^ 3 - 24 * x ^ 2 + 60 * x - 44) / 6
End Function

Private Function cubSpline4(x As Double) As Double
    cubSpline4 = -(x ^ 3 - 12 * x ^ 2 + 48 * x - 64) / 6
End Function

Private Function Ent(x As Double) As Integer
    Ent = Round(x) + Sgn(x - Round(x) - Abs(x - Round(x)))
End Function
```

Bibliography

[1] R. Bartels, J. Beatty, B. Barsky, *An Introduction to Splines for use in Computer Graphics and Geometric Modeling*, Morgan Kaufman Publishers, 1987

[2] Y. Bidel, *Piegeage et refroidissement laser du Strontium - Etude de l'effet des interferences en diffusion multiple*, PhD Thesis, Universite de Nice, 2002

[3] A. Browaeys, *Piegeage magnetique d'un gaz d'helium metastable : vers la condensation de Bose-Einstein*, PhD Thesis, Universite Paris Sud, 2000

[4] C. Cohen-Tannoudji, *Cours de physique atomique et moleculaire: condensats de Bose-Einstein dans un gaz sans interactions*, 1997-98
Website: www.lkb.ens.fr/cours/college-de-france/1997-98/1997-98.htm

[5] W. Ketterle, D.S Durfee, D. Stamper-Kurn, *Making, probing and understanding Bose-Einstein Condensates*, in M. Inguscio, S. Stringari and C.E Wieman editions,

[6] S. Roman, R. Petrusha, P. Loman, *VB.NET language in a Nutshell: a desktop quick reference*

[7] F. Mandl, *Statistical Physics*, Wiley, Second Edition 1998

[8] J. Moore, C. Davis, M. Coplan, *Building Scientific Apparatus - A practical Guide to Design and Construction*, Perseus Books, Second Edition, 1991

[9] H. Metcaolf, P. van de Straten, *Laser Cooling and Trapping*, Springer Verlag, 1991

[10] D. Stamper-Kurn, *Peeking and poking at a new quantum fluid: studies of a gaseous Bose-Einstein Condensates in magnetic and optical traps*, PhD Thesis, MIT, 2000

[11] M. Unser, *Splines, a Perfect Fit for Signal and Image Processing*, IEEE Signal Processing Magazine (1999), 1053-5388

[12] M. Unser, P. Thevenaz, L. Yaroslavsky, *Convolution-Based Interpolation for Fast, High-Quality Rotation of Images*, IEEE Transactions on Image Processing, Vol. 4, NO. 10. October 1995

[13] M. Unser, A. Aldroubi, M. Eden, *Fast-B-Spline Transforms for Continuous Image Representation and Interpolation*, IEEE Transactions on pattern Analysis and Machine Intelligence, Vol. 13, NO. 3. March 1991

[14] Website: www.dbs.c.u-tokyo.ac.jp/~torii/bec/tutorial/chapter2_1.html

[15] Website: www.mpq.mpg.de/qdynamics/projects/bec/BECtrap.html

[16] Website: wlap.physics.lsa.umich.edu/umich/phys/satmorn/2002/20021123/real/sld003.htm

[17] Website: hyperphysics.phy-astr.gsu.edu/hbase/optmod/imgopm/acoum.gif

[18] Website: www.cas.muohio.edu/~meicenrd/sem/pumps.htm

[19] Website: is389-proj-collaps.web.cern.ch/.../SpinPol.htm